



NAVAL POSTGRADUATE SCHOOL

MONTEREY, CALIFORNIA

THESIS

**DETECTION OF A LOW POWER COMMUNICATION
SIGNAL IN THE PRESENCE OF A STRONG CO-
CHANNEL TV BROADCAST INTERFERENCE USING A
KALMAN FILTER**

by

Attique Sajid

December 2014

Thesis Advisor:
Thesis Co-Advisor:

Roberto Cristi
Monique P. Fargues

Approved for public release; distribution is unlimited

THIS PAGE INTENTIONALLY LEFT BLANK

REPORT DOCUMENTATION PAGE			<i>Form Approved OMB No. 0704-0188</i>	
Public reporting burden for this collection of information is estimated to average 1 hour per response, including the time for reviewing instruction, searching existing data sources, gathering and maintaining the data needed, and completing and reviewing the collection of information. Send comments regarding this burden estimate or any other aspect of this collection of information, including suggestions for reducing this burden, to Washington headquarters Services, Directorate for Information Operations and Reports, 1215 Jefferson Davis Highway, Suite 1204, Arlington, VA 22202-4302, and to the Office of Management and Budget, Paperwork Reduction Project (0704-0188) Washington, DC 20503.				
1. AGENCY USE ONLY (Leave blank)		2. REPORT DATE December 2014	3. REPORT TYPE AND DATES COVERED Master's Thesis	
4. TITLE AND SUBTITLE DETECTION OF A LOW POWER COMMUNICATION SIGNAL IN THE PRESENCE OF A STRONG CO-CHANNEL TV BROADCAST INTERFERENCE USING A KALMAN FILTER			5. FUNDING NUMBERS	
6. AUTHOR(S) Attique Sajid			8. PERFORMING ORGANIZATION REPORT NUMBER	
7. PERFORMING ORGANIZATION NAME(S) AND ADDRESS(ES) Naval Postgraduate School Monterey, CA 93943-5000			10. SPONSORING/MONITORING AGENCY REPORT NUMBER	
9. SPONSORING /MONITORING AGENCY NAME(S) AND ADDRESS(ES) N/A			10. SPONSORING/MONITORING AGENCY REPORT NUMBER	
11. SUPPLEMENTARY NOTES The views expressed in this thesis are those of the author and do not reflect the official policy or position of the Department of Defense or the U.S. Government. IRB Protocol number ____N/A____.				
12a. DISTRIBUTION / AVAILABILITY STATEMENT Approved for public release; distribution is unlimited			12b. DISTRIBUTION CODE A	
13. ABSTRACT (maximum 200 words) This research focuses on the detection of a low power communication signal in the presence of a strong co-channel television broadcast interference signal. The presence of strong co-channel interference makes the recovery of the desired weak power signal impossible using conventional filtering techniques that are based on time and frequency characteristics of the signals. The second-generation digital video broadcasting terrestrial (DVB-T2) standard is employed as co-channel interference in an additive white Gaussian noise channel. The weak signal is assumed to have a considerably smaller bandwidth than the TV interference and negligible phase-shift due to multipath. By using two antennas at the receiver, channel diversity can be exploited, and the weak signal can be recovered using a Kalman filter (KF), assuming the channels seen by the two antennas are independent and time-invariant. Moreover, the transmitted co-channel interference is modeled as the state of a dynamic system whose input is the signal received at one antenna and the output is the signal received at the second antenna. Within this framework, the state can be estimated by a KF. Channel estimation is performed using DVB-T2 pilots. Performance of the system is evaluated at different signal-to-noise ratio (SNR) and signal-to-interference ratio (SIR). Results show that the weak signal can be reconstructed with bit error ratio (BER) of 10 ⁻³ or less under most SNR and SIR conditions considered in the study.				
14. SUBJECT TERMS orthogonal frequency-division multiplexing (OFDM), digital video broadcasting-terrestrial (DVB-T), kalman filter, co-channel interference, signal-to-noise , signal-to-interference, channel estimations, communication, second generation digital video broadcasting-terrestrial (DVB-T2)			15. NUMBER OF PAGES 77	
			16. PRICE CODE	
17. SECURITY CLASSIFICATION OF REPORT Unclassified	18. SECURITY CLASSIFICATION OF THIS PAGE Unclassified	19. SECURITY CLASSIFICATION OF ABSTRACT Unclassified	20. LIMITATION OF ABSTRACT UU	

THIS PAGE INTENTIONALLY LEFT BLANK

Approved for public release; distribution is unlimited

**DETECTION OF A LOW POWER COMMUNICATION SIGNAL IN THE
PRESENCE OF A STRONG CO-CHANNEL TV BROADCAST INTERFERENCE
USING A KALMAN FILTER**

Attique Sajid
Lieutenant Commander, Pakistan Navy
BE, Pakistan Navy Engineering College, National University of Science & Technology, 2006

Submitted in partial fulfillment of the
requirements for the degree of

MASTER OF SCIENCE IN ELECTRICAL ENGINEERING

from the

**NAVAL POSTGRADUATE SCHOOL
December 2014**

Author: Attique Sajid

Approved by: Roberto Cristi
Thesis Advisor

Monique P. Fargues
Thesis Co-Advisor

R. Clark Robertson
Chair, Department of Electrical and Computer Engineering

THIS PAGE INTENTIONALLY LEFT BLANK

ABSTRACT

This research focuses on the detection of a low power communication signal in the presence of a strong co-channel television broadcast interference signal. The presence of strong co-channel interference makes the recovery of the desired weak power signal impossible using conventional filtering techniques that are based on time and frequency characteristics of the signals. The second-generation digital video broadcasting terrestrial (DVB-T2) standard is employed as co-channel interference in an additive white Gaussian noise channel. The weak signal is assumed to have a considerably smaller bandwidth than the TV interference and negligible phase-shift due to multipath.

By using two antennas at the receiver, channel diversity can be exploited, and the weak signal can be recovered using a Kalman filter (KF), assuming the channels seen by the two antennas are independent and time-invariant. Moreover, the transmitted co-channel interference is modeled as the state of a dynamic system whose input is the signal received at one antenna and the output is the signal received at the second antenna. Within this framework, the state can be estimated by a KF. Channel estimation is performed using DVB-T2 pilots. Performance of the system is evaluated at different signal-to-noise ratio (SNR) and signal-to-interference ratio (SIR). Results show that the weak signal can be reconstructed with bit error ratio (BER) of 10^{-3} or less under most SNR and SIR conditions considered in the study.

THIS PAGE INTENTIONALLY LEFT BLANK

TABLE OF CONTENTS

I.	INTRODUCTION.....	1
A.	BACKGROUND	1
B.	OBJECTIVE	1
C.	RELATED WORK	2
D.	APPROACH.....	2
E.	THESIS ORGANIZATION.....	3
II.	DVB-T2 STRUCTURE	5
A.	DIGITAL TELEVISION	5
B.	ORTHOGONAL FREQUENCY-DIVISION MULTIPLEXING.....	7
1.	Baseband Implementation	9
2.	Guard Interval	12
3.	CP-OFDM.....	12
4.	DVB-T2	14
5.	DVB-T2 Structure.....	14
6.	DVB-T2 Pilots.....	15
7.	Implementation	16
III.	KALMAN FILTER APPLICATION TO MULTI-ANTENNA SYSTEMS	19
A.	ESTIMATION.....	19
B.	ESTIMATION TECHNIQUES.....	20
C.	THE KALMAN FILTER.....	20
1.	Prediction.....	21
2.	Correction.....	22
3.	Riccati Equation.....	22
D.	KALMAN FILER ESTIMATION OF MULTI-ANTENNA SYSTEMS.....	23
IV.	SIMULATION AND RESULTS	29
A.	SIMULINK IMPLEMENTATION.....	32
1.	Signal-to-Noise Ratio and Signal-to-Interference Ratio.....	32
2.	Estimated CIR.....	33
B.	SIMULATION RESULTS	34
1.	Signal Attenuation	34
a.	<i>Interference Attenuation</i>	35
b.	<i>Signal of Interest Attenuation</i>	36
c.	<i>Noise Attenuation.....</i>	37
2.	DVB-T2 BER Performance Analysis	38
3.	Weak Signal BER Performance Analysis	40
V.	CONCLUSIONS AND RECOMMENDATIONS.....	43
APPENDIX.\	MATLAB CODE	45
LIST OF REFERENCES		53
INITIAL DISTRIBUTION LIST		55

THIS PAGE INTENTIONALLY LEFT BLANK

LIST OF FIGURES

Figure 1.	Block diagram for extraction of the weak signal using a KF.	4
Figure 2.	Map of digital terrestrial television broadcast standards, from [5].	6
Figure 3.	SCM and MCM, from [6].	8
Figure 4.	Block diagram of an MCM modulation scheme.	8
Figure 5.	Block diagram of OFDM modulator, from [5].	11
Figure 6.	Effect of τ and GI on ISI.	12
Figure 7.	Illustration of CP-OFDM.	13
Figure 8.	DVB-T2 frame structure, showing the division into superframes, T2 frames, and OFDM symbols, after [7].	15
Figure 9.	Pilot pattern used in DVB-T2.	16
Figure 10.	Block diagram of DVB-T2 implementation in Simulink.	17
Figure 11.	One cycle of KF state estimation, from [8].	23
Figure 12.	Transfer function approach to estimate state of transmitted data.	28
Figure 13.	Frequency domain plot of interferer (y_2), weak signal (s) and noise (w) for SNR=20 dB and SIR= - 25 dB.	29
Figure 14.	Block diagram for recovering weak signal.	30
Figure 15.	Suppression of interference and recovery of weak signal for SNR=20 dB and SIR= - 25 dB.	31
Figure 16.	Recovered weak signal (\hat{s}) after demodulation for SNR=20 dB and SIR= - 25 dB.	31
Figure 17.	Attenuation of the interference y_1 for different noise power levels and error percentages in the estimated CIR coefficients.	35
Figure 18.	Attenuation of the interference y_2 for different noise power levels and error percentages in the estimated CIR coefficients.	36
Figure 19.	Attenuation of the signal s for different noise power levels and error percentages in the estimated CIR coefficients.	37
Figure 20.	Attenuation of the noise w for different noise power levels and error percentages in the estimated CIR coefficients.	38
Figure 21.	DVB-T2 Channel 1 signal BER at different SIR.	39
Figure 22.	DVB-T2 Channel 2 signal BER at different SIR.	39
Figure 23.	Weak signal BER with SIR= - 5 dB and 15% error in estimated CIR coefficients.	40

THIS PAGE INTENTIONALLY LEFT BLANK

LIST OF TABLES

Table 1.	Parameters used in DVB-T2 standard.....	14
----------	---	----

THIS PAGE INTENTIONALLY LEFT BLANK

LIST OF ACRONYMS AND ABBREVIATIONS

ATSC	Advanced Television Systems Committee
AWGN	additive white Gaussian noise
BCH	Bose-Chaudhuri-Hocquengham
bps	bits per second
CIR	channel impulse response
CP-OFDM	cyclic prefix orthogonal frequency-division multiplexing
DFT	discrete Fourier transform
DTMB	digital terrestrial multimedia broadcast
DTV	digital television
DVB-T2	second generation digital video broadcasting – terrestrial
FDM	frequency-division multiplexing
FEC	forward error correction
FFT	fast Fourier transform
GI	guard interval
HDTV	high definition television
ICA	independent component analysis
IDFT	inverse discrete Fourier transform
IFFT	inverse fast Fourier transform
ISDB-T	integrated services digital broadcasting – terrestrial
ISI	inter symbol interference
KF	Kalman filter
LDPC	low density parity check
LSE	least squares estimator
MCM	multicarrier modulation
NTSC	national television systems committee
OFDM	orthogonal frequency-division multiplexing
PAL	phase alternating line
POI	parameter of interest
QAM	quadrature amplitude modulation
QPSK	quadrature phase-shift keying

SCM	single carrier modulation
SDTV	standard definition television
SIR	signal-to-interference ratio
SNR	signal-to-noise ratio
sps	symbols per second
TV	television

EXECUTIVE SUMMARY

Most conventional signal processing techniques used in receivers focus on signal time and frequency characteristics to recover transmitted information. In such cases, signal information can only be recovered if its power is greater than the combined power of the noise and interferences; however, military and commercial application scenarios exist in which the desired signal is transmitted in the presence of much stronger co-channel interference signal.

The objective of this thesis is to recover a signal embedded in strong co-channel broadcasting interference signal. The overhead information of the broadcasting signal (typically used for detection and synchronization tasks) is used in a multi-antenna system to estimate the multipath and time delay characteristics, allowing for a relatively simple interference cancellation algorithm based on Kalman filtering (KF) techniques. The technique presented is novel and may open the possibility of using the frequency spectrum occupied by digital video and radio broadcasting for other purposes, such as low power data transmission.

The approach considered in this work is based on a two-antenna model at the receiver and relies on channel diversity at the two receiving antennas. The main assumptions of this approach are:

1. The weak signal is minimally affected by multipath.
2. The knowledge of the interferer's overhead is sufficient to estimate the transmission channel parameters.

These conditions can be satisfied by placing the two antennas at least half a wavelength apart and keeping the weak signal bandwidth smaller than the frequency coherence of the channel.

In this research, the strong signal interferer is assumed to be a second-generation digital video broadcasting-terrestrial (DVB-T2) signal, which is based on orthogonal frequency-division multiplexing (OFDM), and the weak signal is a quadrature phase-shift keying (QPSK) single-carrier modulated signal. The DVB-T2 signal passes through two

multipath channels with additive white Gaussian noise (AWGN). Estimation of the two channels is conducted using the pilots present in the DVB-T2 signal.

The proposed approach is based on the KF and uses the signals received at the two antennas and estimated channel coefficients to estimate the DVB-T2 signal interferer. By this particular structure, adapted from the controls literature, the two signals received at the antennas, respectively, act as predictor and corrector of the state of a dynamic system, where the state represents the transmitted TV broadcasted signal. What the KF literature calls the innovation, contains the unpredictable part of the dynamic model, from which the weak signal can be recovered and demodulated using a standard QPSK demodulator. This concept is illustrated in Figure 1.

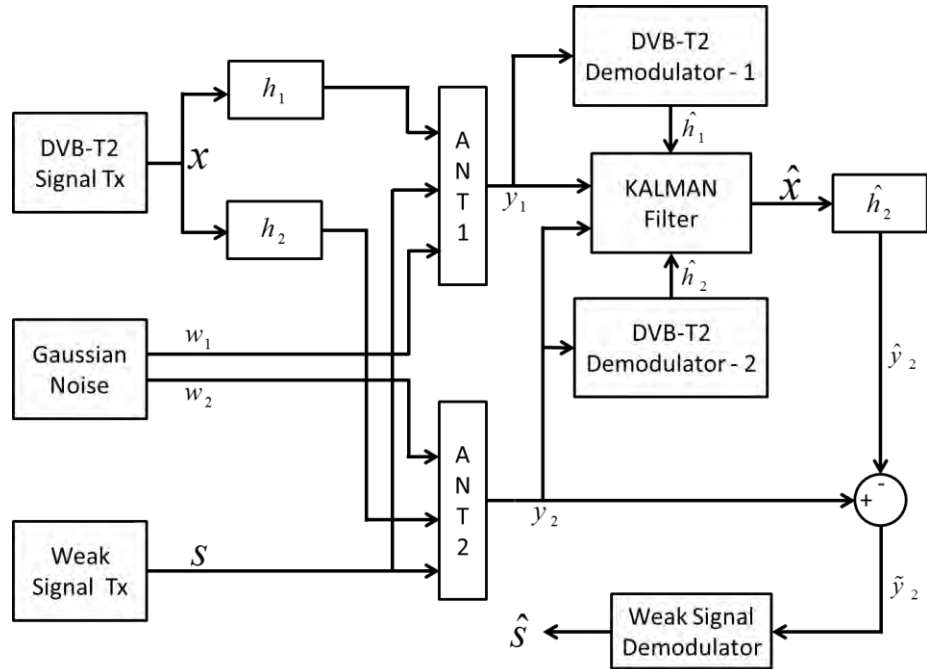


Figure 1. Block diagram of the KF approach used to recover the weak signal

The estimated channel impulse responses (CIRs) are used both for equalization in the respective DVB-T2 receivers and in the KF to estimate the state of the DVB-T2 signal.

Results show that the weak signal can be extracted from the interference and noise when the underlying assumptions of the scheme presented in the research are met. Both interference and weak signals can be demodulated with bit error ratio (BER) values of 10^{-3} or less under most signal-to-noise ratio (SNR) and signal-to-interference ratio (SIR) conditions investigated. Follow-on research should include a robust approach for estimating the channel characteristics to allow for better BER performances.

THIS PAGE INTENTIONALLY LEFT BLANK

ACKNOWLEDGMENTS

And say: My Lord increase me in knowledge.

–Qur'an, Ta-Ha 20:114

Read! In the name of your Lord who created – Created the human from something which clings. Read! And your Lord is Most Bountiful – He who taught (the use of) the Pen, Taught the human that which he knew not.

–First revealed verses of Qur'an, Al-Alaq 96:1-5

First and foremost, I would thank Almighty Allah for bestowing upon me the opportunity to seek a master's degree at the Naval Postgraduate School and providing me the wisdom and perseverance to complete both the course and research work.

I would like to express thanks to Professor Cristi, my thesis advisor. His continuous support, guidance and advice are what made this thesis possible. He is one of the most inspirational instructors I ever had, and I appreciate all the contributions he made to make my stay at NPS a wonderful learning experience. I would also like to thank Professor Fargues for patiently proofreading my thesis drafts over again. Without her support, I would not have been able to present the thesis in its current form.

I would also like to thank ECE Signal Processing, Communications and Electronics faculty who put their best effort to guide us to the path of seeking knowledge. It will be injustice not to mention my ECE colleagues, who provided the perfect atmosphere to make this learning truly a memorable experience.

I would like to express my gratitude to my family members back home for their love and encouragement. My parents deserve special thanks for their unconditional love and support in all my pursuits. Their persistent emotional support throughout my stay always inspired me to keep working hard and made them proud.

Finally, I recognize the support of my wife, Mahwish, and my son, Wamiq. Their affection and love, particularly in the final stages, is greatly appreciated.

THIS PAGE INTENTIONALLY LEFT BLANK

I. INTRODUCTION

A. BACKGROUND

In most communications systems, conventional signal processing techniques used in receivers focus on time and frequency characteristics of the signals to recover the transmitted information. In such cases, the signal can only be recovered if its power is sufficiently greater than that of the noise and interference; however, there may be cases when the desired signal power is considerably lower (whether intentionally or unintentionally) and is transmitted in the presence of strong co-channel interference. Such situations can be encountered in both military and commercial systems. For example, military communication systems may experience strong co-channel jamming, which denies the reception of a desired signal. Similarly, in the commercial world, if a communication system can operate reliably in the presence of a strong, co-channel interference, then there is no need to buy spectrum, an expensive commodity.

In this thesis we address the problem of recovering a communication signal in the presence of a strong co-channel interferer. In particular, we show that using a priori knowledge of the interferer (e.g., its overhead and a multi-antenna receiver) the interferer can be estimated and highly attenuated by cancellation.

B. OBJECTIVE

The objective of this thesis is to recover a signal from a co-channel interference signal. In this case, classical filtering techniques cannot be applied, as both signals occupy the same frequency bands. The signal-of-interest is extracted by taking advantage of the known overhead portion (commonly used for detection and synchronization) contained in the interferer, selected to be a broadcast signal. This overhead information can be used in a multi-antenna system to estimate the transmission channel multipath and time delay characteristics, which leads to a relatively simple interference cancellation scheme based on Kalman filtering techniques.

The technique presented in this work is novel and may open the possibility of using the frequency spectrum occupied by digital video and radio broadcasting for other purposes, such as low power data transmission.

C. RELATED WORK

The co-channel interference problem has been investigated recently for various kinds of settings. One approach has been based on Independent Component Analysis (ICA), where the signals' statistical properties are used for separation purposes [1]. Algorithms based on ICA were presented in [2] which show the effectiveness of the technique in cases with no multipath.

The use of Kalman Filtering in a multi-antenna system has recently been introduced in [3] and [4]. The use of the Kalman Filter (KF) for this particular application has not been widely published and seems to yield an interesting framework for recovering data from a multi-antenna system. Formulating the multi-antenna receiver as a state space dynamic system, widely used in the controls systems literature, allows for the application of well-known state estimation techniques, such as the state observer and the KF.

D. APPROACH

The approach employed in this research is based on a two-antenna model at the receiver and relies on the presence of channel diversity at the two receiving antennas. This means that the signal reaching each antenna sees a different channel. The main assumptions of this approach are the following:

1. The weak signal is minimally affected by the multipath.
2. Knowledge of the interferer's overhead allows for the estimation of the transmission channel parameters.

These conditions can be satisfied by placing the two antennas at least half a wavelength apart and keeping the weak signal bandwidth smaller than the frequency coherence of the channel.

The strong signal interferer is assumed to be a second generation digital video broadcasting–terrestrial (DVB-T2) signal, which is the European television (TV) standard. DVB-T2 is based on orthogonal frequency-division multiplexing (OFDM). The weak signal is modeled as a quadrature phase-shift keying (QPSK), single-carrier modulated signal. The DVB-T2 signal passes through two additive white Gaussian noise (AWGN) channels. Estimation of the two channels characteristics is conducted via the pilots present in the DVB-T2 signal.

The proposed approach is based on the KF algorithm and uses the signals received at the two antennas and estimated channels characteristics to estimate the DVB-T2 signal interferer. By this particular structure, adapted from the controls literature, the two signals received at the antennas act as predictor and corrector of the state of a dynamic system, where the state represents the transmitted TV broadcasted signal. What is called the “innovation” in the KF literature contains what cannot be predicted by the dynamic model, from which the weak signal can be recovered and demodulated using a standard QPSK demodulator. This concept is illustrated in Figure 1. The performance of the system is evaluated at different signal-to-noise ratio (SNR) and signal-to-interference ratio (SIR) values.

E. THESIS ORGANIZATION

This thesis is organized into five chapters including the introduction. The basic idea behind the DVB-T2 structure is explained in Chapter II to highlight the estimation process of the channel impulse response (CIR). The KF algorithm and its application to the proposed scheme are presented in Chapter III. The discussion in Chapter IV focuses on the simulation model and results obtained at different SNRs and SIRs. Finally, conclusions and recommendations are provided in Chapter V.

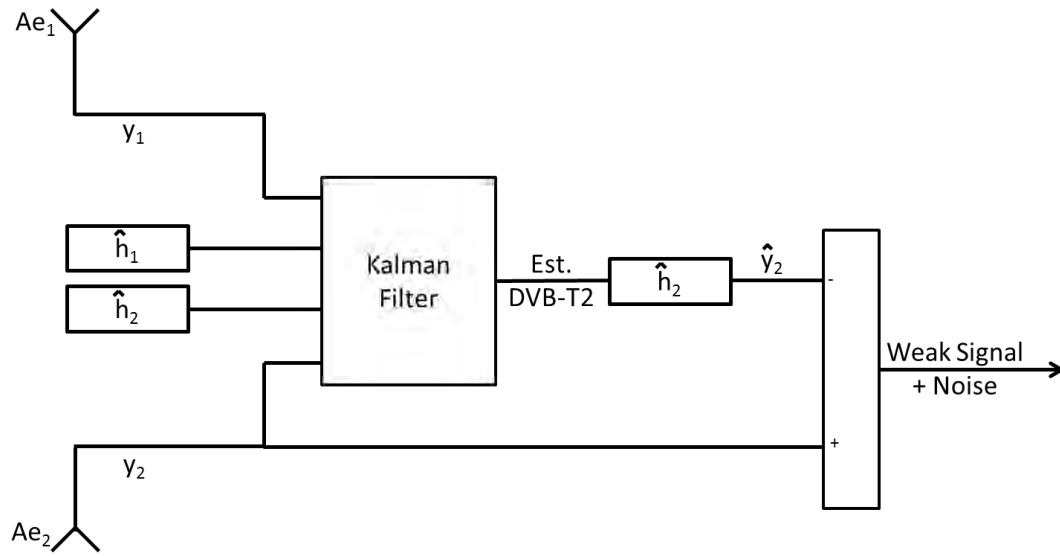


Figure 1. Block diagram for extraction of the weak signal using a KF.

II. DVB-T2 STRUCTURE

We have seen the evolution TV has undergone over the last couple of decades. The video which we see on standard definition television (SDTV) follows standards that were developed in the 1940s and 1950s. The two most widely used analog standards are the national television systems committee (NTSC) and phase alternating line (PAL). NTSC is the dominant standard on the American continent and Japan, while PAL is the one for Europe, Asia, and Australia. These two standards have dominated the TV market for almost 60 years. With the advent of the digital age, NTSC and PAL have lost considerable ground to emerging technologies.

Digital TV (DTV) broadcasting concepts are presented in this chapter followed by a brief description of OFDM and its implementation in the DVB-T2 standard. Finally, we describe the approach followed to extract channel characteristics using DVB-T2 pilot signals.

A. DIGITAL TELEVISION

Technology advances have taken huge leaps in the recent past, and tremendous progress has been seen in every field of life. Such advances have resulted in rising demand for fast, efficient, and high throughput systems, and the broadcasting industry is no exception. In order to keep up with the technology and consumer demand, the shift to DTV is a natural evolution. The first DTV service was delivered via satellite, and now this service is provided via terrestrial and cable networks. DTV has many advantages over analog TV. A Few of these advantages include:

- less interference
- better video and audio quality
- multiplexing which allows various types of signals to be transmitted simultaneously
- better spectral efficiency

Due to the inherent versatility of digital transmission, DTV has brought many exciting variations to TV broadcasting, and various digital high-definition TV (HDTV) standards have been adopted all over the world. The most popular ones are:

- advanced Television Systems Committee (ATSC)
- integrated services digital broadcasting – terrestrial (ISDB-T)
- digital video broadcasting (DVB-T)
- digital terrestrial multimedia broadcast (DTMB)

The regions where these standards have been implemented are shown in Figure 2. All these standards follow the same general structure; however, specific implementation schemes differ from standard to standard.



Figure 2. Map of digital terrestrial television broadcast standards, from [5].

The research conducted here considers the case of a strong TV broadcast signal interfering with a signal transmitting at a lower power embedded in the same frequency band. Although the assumption throughout is that the TV broadcast signal has a DVB-T2

structure, the techniques developed are general in nature and can be applied to any standard.

The DVB-T2 standard structure is based on OFDM and employs a number of digital modulation constellations such as QPSK, 16-quadrature amplitude modulation (QAM), 64-QAM, or 256-QAM, and various coding schemes to adapt to different channel and multipath situations.

B. ORTHOGONAL FREQUENCY-DIVISION MULTIPLEXING

In wireless systems, the signal at the receiver comes from different paths due to reflection and diffraction from large objects such as buildings, hills, etc. Each path is characterized by different levels of attenuation and delay; therefore, multiple copies of the same signal are received, delayed, and attenuated, causing inter-symbol interference (ISI).

A wireless channel is characterized by its time spread and frequency spread. The effect of ISI is negligible when the symbol duration of the transmitted signal is considerably higher than the time spread of the channel. This condition corresponds to a flat fading channel scenario; however, equalization is essential to compensate for channel distortions when the transmitted signal symbol duration is smaller than the channel time spread value. This second scenario corresponds to a frequency-selective channel case. Equalization requires training data (thus, loss of bandwidth) that can be computationally expensive if done blindly and is difficult when the channel characteristics are time varying.

In single-carrier modulation (SCM), each bit is transmitted on a single carrier frequency. An alternative approach is to divide the available channel bandwidth into a number of sub-channels each with equal bandwidth. The bandwidth of each channel is selected to be as narrow as possible so that each sub-channel sees a flat fading channel and ISI is minimized. Different information symbols can be transmitted on each sub-channel simultaneously. This scenario is a particular case of frequency-division multiplexing (FDM), known as multicarrier modulation (MCM) in which each sub-

channel is associated with a single carrier. SCM and MCM concepts are illustrated in Figure 3.

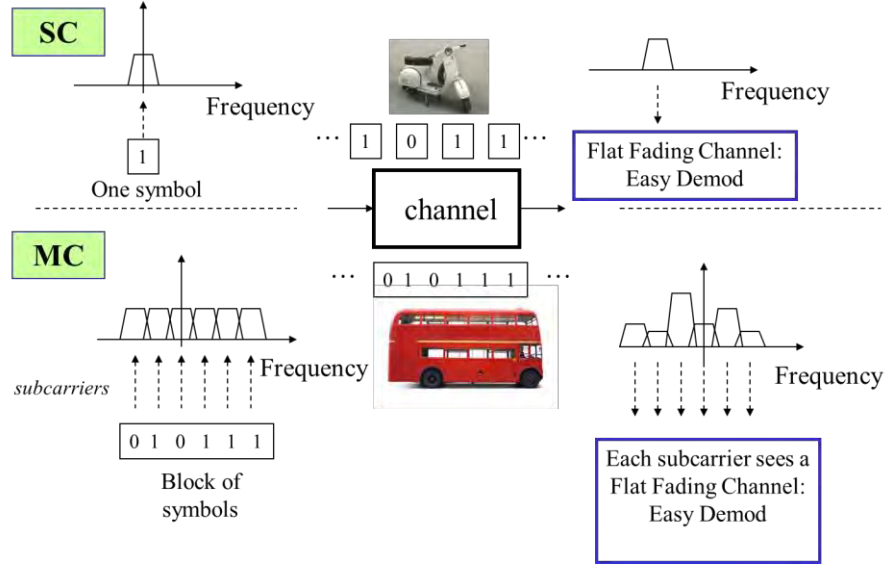


Figure 3. SCM and MCM, from [6].

In SCM, data is transmitted on a single frequency at a higher data rate $R = 1/T$. In MCM, the data is transmitted over N subcarriers at a lower data rate $R/N = 1/NT$, as shown in Figure 4. In such a case, a N -symbol data block can be chosen so that the total time duration NT of the symbol frame is considerably longer than the channel time spread.

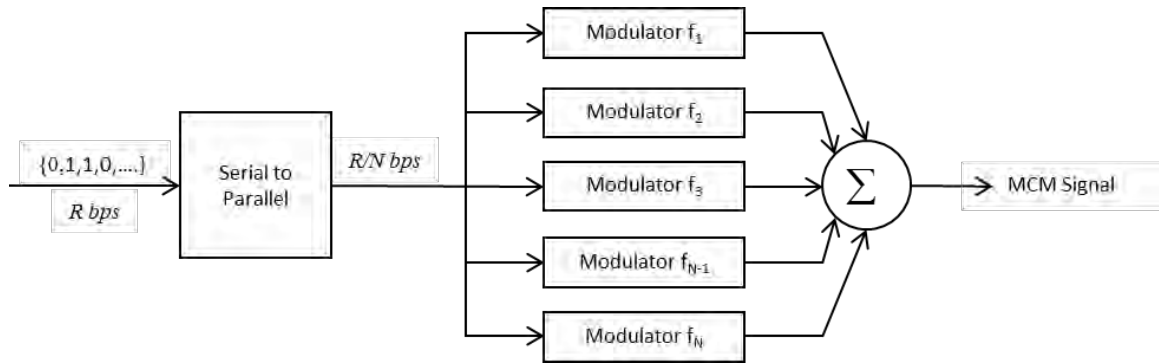


Figure 4. Block diagram of an MCM modulation scheme.

OFDM is a special case of FDM in which all subcarriers are orthogonal to each other and is widely used in wireless systems including the popular IEEE 802.11a, g, n standards, DVB-T2 standard and long-term evolution (LTE) cellular networks. A further advantage of MCM is that the transmission power can be efficiently distributed across subcarriers based on the transmission channel frequency response to maximize the data rate.

As shown in Figure 4, data bits transmitted at a rate $R = 1/T$ bits per second are converted into N streams, each one having a symbol rate F_s of $F_s = 1/NT = 1/T_s$ symbols per second (sps) and independently modulated by one of N orthogonal subcarriers. By separating the subcarriers by $1/T_s$, we guarantee orthogonality so that the transmitted symbols in each time data block do not interfere with each other. Note that it is not feasible to implement the scheme given in Figure 4 due to the large number of modulators used. Instead baseband implementation is considered, which is discussed next [7].

1. Baseband Implementation

It is well known that an OFDM signal is transmitted as a sequence of OFDM frames, each one of duration T_s and where each frame $s(t)$ is the superposition of modulated subcarriers, as given by

$$s(t) = \frac{1}{N} \sum_{k=0}^{N-1} s_k(t), \quad 0 \leq t < T_s, \quad (2.1)$$

where $s_k(t)$ is given by

$$s_k(t) = \text{Re}\{z_k(t)e^{j[2\pi(f_c + k\Delta f)t]}\}, \quad 0 \leq t < T_s, \quad (2.2)$$

with $k = 0, 1, 2, \dots, N-1$, and z_k represents the complex envelope of the k^{th} subcarrier, f_c is the nominal carrier frequency, and $\Delta f = 1/T_s$ is the carrier symbol rate chosen to maintain orthogonality among subcarriers. The complex envelope of the k^{th} subcarrier is given by

$$z_k(t) = Z(k) = I_k + jQ_k, \quad 0 \leq t < T_s, \quad (2.3)$$

where I_k and Q_k represent I, Q values of the k^{th} subcarrier symbol and are the in-phase and quadrature components of $z_k(t)$, respectively.

By substituting Equation (2.2) into Equation (2.1), we get

$$\begin{aligned} s(t) &= \frac{1}{N} \sum_{k=0}^{N-1} \text{Re}\{Z(k)e^{j[2\pi(f_c+k\Delta f)t]}\} = \frac{1}{N} \sum_{k=0}^{N-1} \text{Re}\{Z(k)e^{j2\pi k\Delta f t} e^{j2\pi f_c t}\} \\ &= \text{Re}\left\{\left(\frac{1}{N} \sum_{k=0}^{N-1} Z(k)e^{j2\pi k\Delta f t}\right) e^{j2\pi f_c t}\right\}, \quad 0 \leq t < T_s. \end{aligned} \quad (2.4)$$

Thus, the complex envelope of ODFM signal is given by

$$s_L(t) = \frac{1}{N} \sum_{k=0}^{N-1} Z(k)e^{j2\pi k\Delta f t}, \quad 0 \leq t < T_s. \quad (2.5)$$

Sampling rate and sampling time are given by $F_{\text{sampling}} = NF_s$ and $T_{\text{sampling}} = T_s / N$, which yields the sampled signal expression:

$$s_L\left(\frac{nT_s}{N}\right) = \frac{1}{N} \sum_{k=0}^{N-1} Z(k)e^{j2\pi k\Delta f nT_s/N}, \quad n = 0, 1, \dots, N-1. \quad (2.6)$$

Choosing $\Delta f T_s = 1$ renders the subcarriers orthogonal to each other and yields the well-known expression of the inverse discrete Fourier transform (IDFT)

$$\begin{aligned} s_L(n) &= \frac{1}{N} \sum_{k=0}^{N-1} Z(k)e^{j2\pi kn/N}, \quad n = 0, 1, \dots, N-1 \\ &= \text{IDFT}\{Z(k)\}. \end{aligned} \quad (2.7)$$

It is evident from Equation (2.7) that the sequence $s_L(n)$ can be obtained by taking the IDFT of $Z(k)$ where $k = 0, 1, \dots, N-1$. Conversely, $Z(k)$ can be obtained by taking the discrete Fourier transform (DFT) of the sequence $s_L(n)$, as given by

$$\begin{aligned} Z(k) &= \sum_{n=0}^{N-1} s_L(n)e^{-j2\pi kn/N}, \quad k = 0, 1, \dots, N-1 \\ &= \text{DFT}\{s_L(n)\}. \end{aligned} \quad (2.8)$$

Both DFT and IDFT operations can be computed via very efficient fast Fourier transform (FFT) and inverse fast Fourier transform (IFFT) algorithms, respectively. Therefore, OFDM modulation and demodulation can be implemented using the IFFT and FFT algorithms, respectively, at baseband. In practice, the number of subcarriers N is chosen so that the FFT operation can be implemented efficiently. Although in most implementations a power of four is preferred (all IEEE standards), it is not necessarily the case in all recent implementations, such as in DTMB adopted by the People's Republic of China [8].

A typical implementation of an OFDM modulator via baseband approach is shown in Figure 5. Incoming data bits $\{0, 1\}$ are encoded into M-QAM complex symbols, which are multiplexed into N parallel streams. For the k^{th} bit stream, a group of $\log_2 M$ bits is mapped into a subcarrier symbol $Z(k) = I_k + jQ_k$, $0 \leq k < N$. Next, the sequence of N symbols is fed into the IFFT block to obtain the sequence $s_L(n)$ which represents the samples of the OFDM complex envelope.

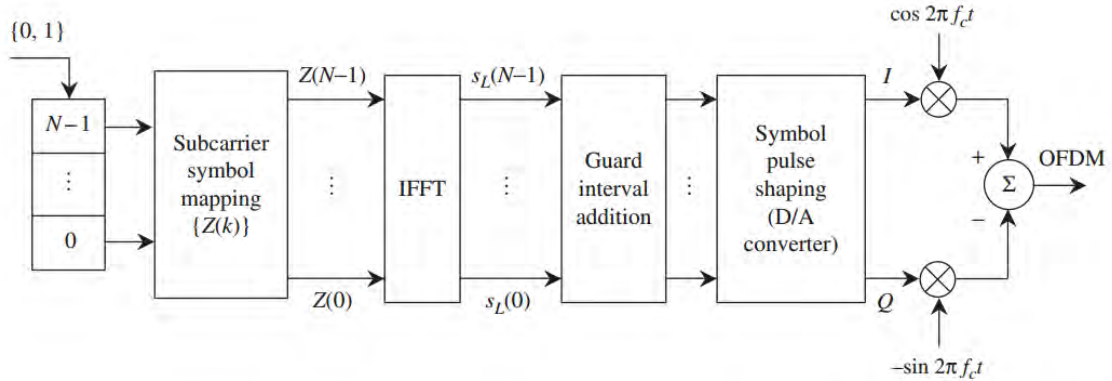


Figure 5. Block diagram of OFDM modulator, from [5].

The digital-to-analog (D/A) converter output is a complex I-Q waveform given by

$$\hat{s}_L(t) = \sum_{k=0}^{N-1} s_L(n) p(t - nT_s / N), \quad (2.9)$$

where $p(t)$ is the interpolation pulse shape, coming from the Zero Order Hold and the low pass reconstruction filter [5].

2. Guard Interval

A guard interval (GI) is added to an OFDM symbol in order to avoid ISI. The GI duration T_g is chosen so that $T_g > \tau_{\max}$ where τ_{\max} is the maximum time spread of the channel. At the receiver, GI is removed before the FFT operation. Adding GI decreases the throughput of the system because no new information is present in the GI. The effect of τ and GI on ISI is shown in Figure 6. It can be seen that ISI cannot be eliminated when $T_g < \tau$.

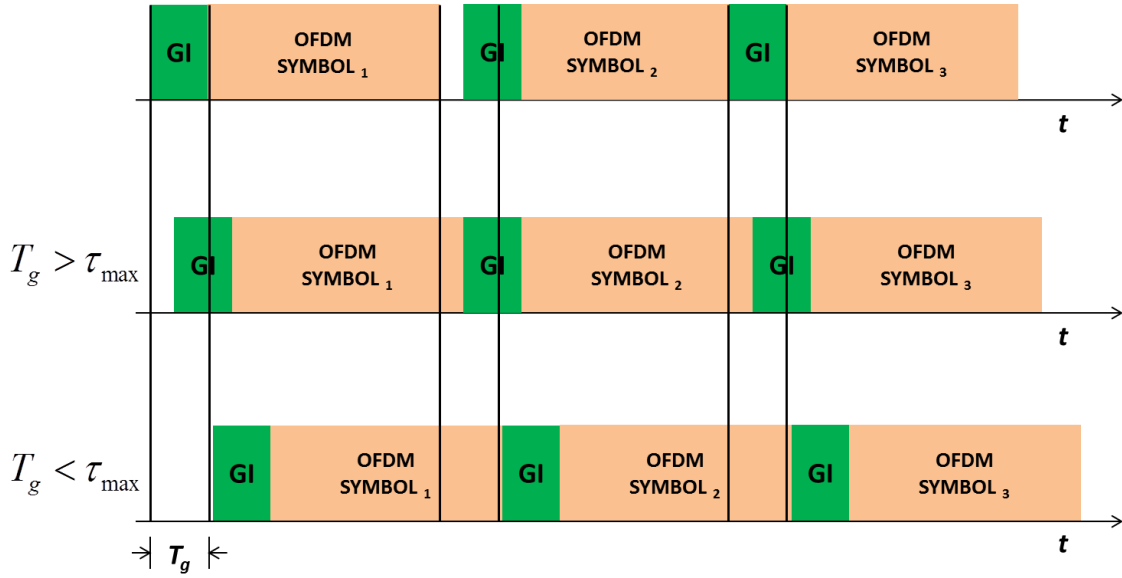


Figure 6. Effect of τ and GI on ISI.

Various OFDM-based techniques have been established based on the structure of the data used in GI. Among them, Cyclic prefix (CP-OFDM), zero prefix (ZP-OFDM), known symbol padding (KSP-OFDM) and time-domain synchronous (TDS-OFDM) are the most widely used. Next, we discuss CP-OFDM as it is used in DVBT-2.

3. CP-OFDM

In this technique, the GI data is created by repeating the last L entries of each OFDM frame, so that LT_s exceeds the time spread of the channel, as shown in Figure 7.

This constraint forces periodic boundary conditions, and it can be easily shown that each received OFDM frame is the result of a circular convolution between the transmitted frame and CIR, thus making the use of the FFT appropriate [5].

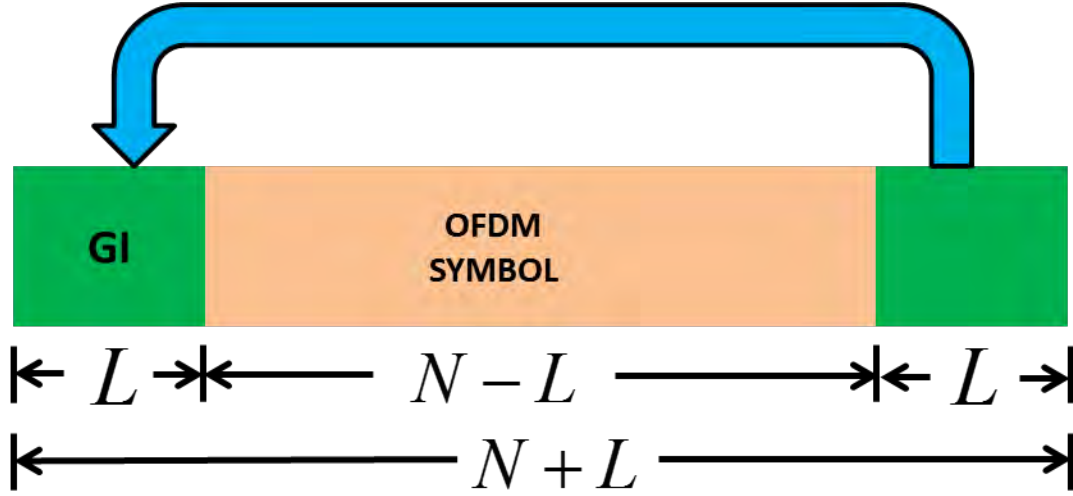


Figure 7. Illustration of CP-OFDM.

Next, demodulation of each OFDM frame is obtained by discarding the first L samples, eliminating inter block interference, and then taking the N -point DFT of the remaining samples. This operation yields

$$Y(k) = H(k)X(k), \quad k = 0, 1, \dots, N-1, \quad (2.10)$$

where $H(k)$ is the N -point DFT of the CIR. Therefore, the CIR can be determined by transmitting training data at the beginning of the transmission and tracked by reserving some subcarriers as pilots so that the transmitted data $Z(k)$ can be estimated.

The approach considered in this work to separate the desired signal from the TV broadcasting interferer makes full use of the information contained in the DVB-T2 signal's overhead. Such overhead information is readily available and easy to demodulate since broadcasting systems are designed for mass production and require quick synchronization at the receivers.

In this section, we present the characteristics of the DVB-T2 system with particular attention to the overhead, which contains the necessary information for

synchronization, channel estimation, and demodulation. As is seen in following chapters, the proposed system is very efficient in the sense that it makes minimal use of the overhead without the need to demodulate the complete broadcast signal.

4. DVB-T2

DVB-T2 uses coded OFDM (COFDM) with a large number of subcarriers and employs different modulation schemes along with inner low density parity check (LDPC) coding combined with outer Bose-Chaudhuri-Hocquengham (BCH) coding. The number of carriers, GI sizes, and pilot signals can be adjusted. Some of the adjustable parameters are given in Table 1. Full details of the DVB-T2 standard can be found in [9].

Table 1. Parameters used in DVB-T2 standard.

FEC	LDPC + BCH 1/2, 3/5, 2/3, 3/4, 4/5, 5/6
Modes	QPSK, 16-QAM, 64-QAM, 256-QAM
GI	1/4, 19/128, 1/8, 19/256, 1/16, 1/32, 1/128
FFT size	1k, 2k, 4k, 8k, 16k, 32k
Scatter pilots	1%, 2%, 4%, 8% of total
Continual pilots	0.4%-2.4% (0.4% - 0.8% in 8k-32k)
Bandwidth	1.7, 5, 6, 7, 8, 10 MHz

5. DVB-T2 Structure

DVB-T2 frame structure is shown in Figure 8. At the top level, there are superframes that consist of T2 frames, which are further divided into OFDM symbols. The number of T2 frames in a super frame is a configurable parameter.

Preamble P1 symbols are used for fast detection of the T2 signal and identification of its parameters from the preamble to enable proper synchronization and demodulation at the receiver. The P2 symbol(s) follow immediately after the P1 symbol. The main purpose of the P2 symbol(s) is to carry L1 signaling data which define the various parameters used for the transmission [9].

Each T2 frame comprises of one P1 preamble symbol, followed by one or more P2 preamble symbols, followed by a configurable number of data symbols.

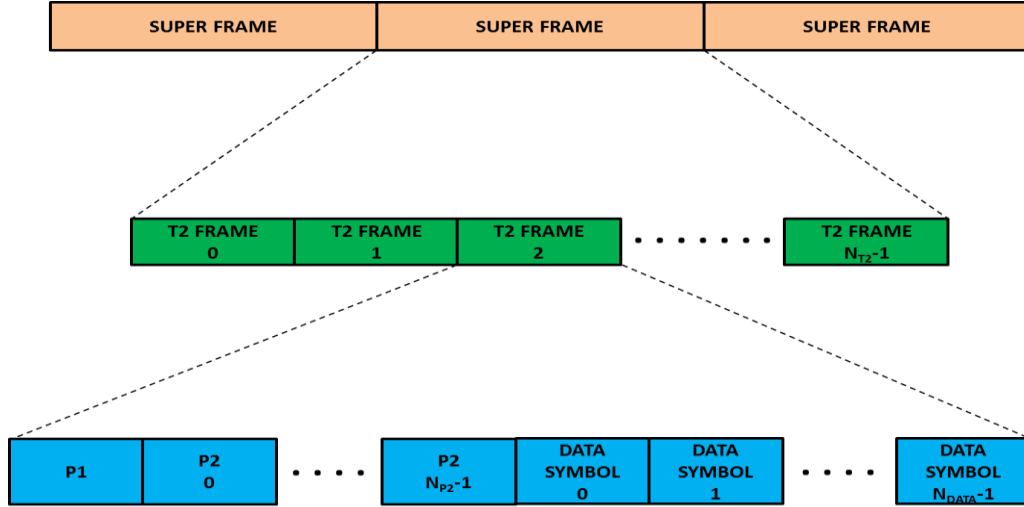


Figure 8. DVB-T2 frame structure, showing the division into superframes, T2 frames, and OFDM symbols, after [7].

6. DVB-T2 Pilots

Various cells within the OFDM frame are modulated with reference information whose transmitted value is known to the receiver. These are called pilots and are transmitted at boosted power level. Pilots can be used for frame synchronization, frequency synchronization, time synchronization, channel estimation, transmission mode identification and can also be used to compensate for hardware limitations, such as phase noise [9].

Data and overhead subcarriers are periodically allocated in time and frequency so that channel variations can be tracked efficiently with minimal loss of data bandwidth. Frequency allocations of data and overhead subcarriers are shown in Figure 9. The subcarriers reserved for overhead are subdivided into pilots (continual and scattered), P2 symbols for defining various parameters used for the transmission and frame-closing symbols for quick synchronization. All other subcarriers contain data. Of particular interest are the scattered pilots, which cover a sufficient range of frequencies so that the channel's frequency response can be easily determined by interpolation.

The locations of continual pilots are fixed from symbol to symbol, and those of scattered pilots change from symbol to symbol. Further details on the distribution of pilots are provided in [9]. One of the pilot patterns used in DVB-T2 signal is shown in Figure 9.

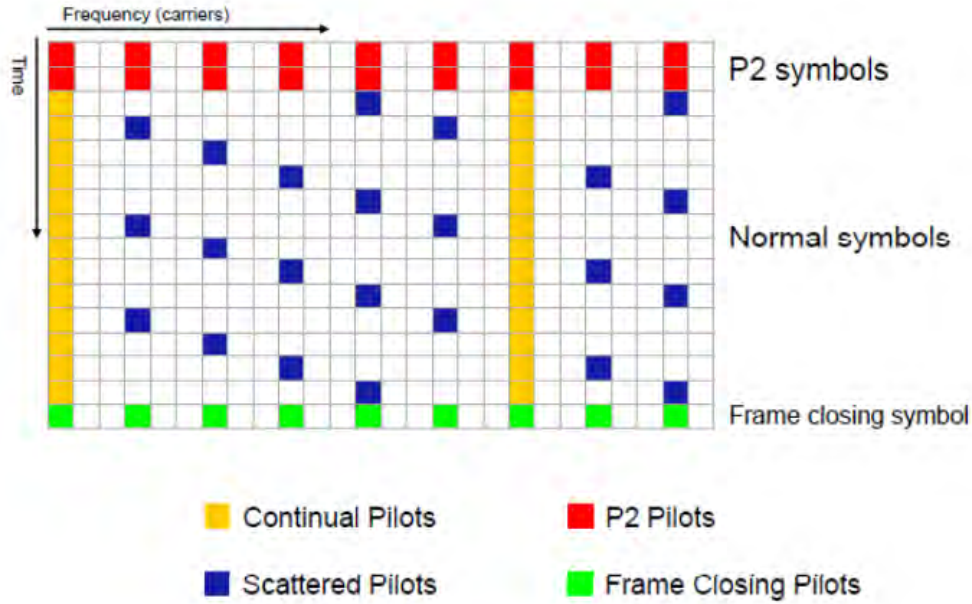


Figure 9. Pilot pattern used in DVB-T2.

7. Implementation

DVB-T2 includes many configurable parameters, as discussed previously. A Simulink model was developed for the modulator and demodulator functions using the configuration discussed next. Each superframe consists of four T2 frames, and each T2 frame consists of 68 OFDM symbols. In particular, in what is called the “2K mode,” for each OFDM symbol there are 1,512 data subcarriers, 343 nulls, 176 pilot subcarriers, and 17 P2-subcarriers, for 2,048 subcarriers. The distribution of pilot subcarriers changes cyclically from OFDM Symbol 0 to OFDM Symbol 67. Scattered and continual pilots overlap at ten locations to make 176 pilots.

The GI length varies with the FFT size. For example, for the 2K mode, GI choices are 1/32, 1/16, and 1/4 [9]. In the case of a 2048-point FFT with GI choice of 1/32,

presented in this research, each OFDM symbol has a total of $2048 + 2048/32 = 2112$ samples. The modulation scheme for data is QPSK, and M-QAM, with M varying from 16 to 256. For our simulations, QPSK was chosen for data, while pilot subcarriers are transmitted using BPSK. The block diagram of the DVB-T2 structure implemented during simulation is shown in Figure 10.

The proposed demodulation scheme is based on the detection and demodulation of the continual and scattered pilots for channel estimation and the frame-closing symbols for fast frame synchronization. This process is an integral part of our model-based demodulation using multiple antennas and Kalman filtering and is presented next. Any other overhead information regarding broadcast data demodulation is irrelevant and disregarded.

Underlying principles of the DVB-T2 standard were presented in this chapter and estimation of transmission CIR characteristics, using pilot signals present within DVB-T2 signal, was also discussed. The approach proposed in this research uses a two-antenna model and requires independence between the two transmission channels to extract the weak signal; therefore, CIRs for both transmission channels are estimated from pilot signals contained in the respective DVB-T2 signals received at each antenna. These two estimated CIRs are then used in a KF framework to estimate the state of DVB-T2 signal, as discussed next in Chapter III.

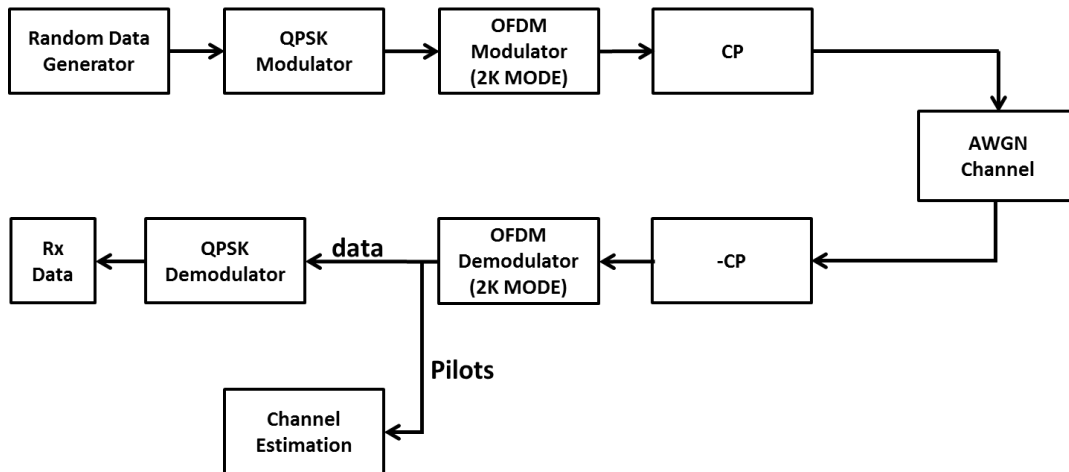


Figure 10. Block diagram of DVB-T2 implementation in Simulink.

THIS PAGE INTENTIONALLY LEFT BLANK

III. KALMAN FILTER APPLICATION TO MULTI-ANTENNA SYSTEMS

The KF and its variants are among the most popular estimation techniques and have applications in almost all fields of technology. This success is due to its simple structure, small computational requirements, recursive nature, robustness, and optimal estimation for linear systems with Gaussian noise. Estimation and different estimation schemes are first discussed in this chapter. Next, the state-space model for a linear dynamic system is described followed by the application of the KF to this model to estimate the state of the system. Finally, application of the KF framework to estimate the state of DVB-T2 signal is discussed.

A. ESTIMATION

Estimation is the process of extracting the value of a parameter-of-interest (POI) from a random, noisy, and uncertain data set of measurements. Noise can arise from sensor measurements, instrument inaccuracies, signal propagation channel or human error and causes randomness in POI as well. The estimator attempts to predict the best estimate of the unknown POI using these noisy measurements. Filtering is the process of eliminating noise (undesirable signals) from noisy measurements in order to obtain the best estimate of the POI. The extraction of the best estimate requires some sort of decision making according to some preset criteria in order to choose the best from a set of alternatives. The criteria can be different for different situations, and an optimal estimator yields the best estimate by optimizing certain criteria. POI can be a random variable, which is time-invariant, or the state of a dynamic system, which is a time-variant stochastic process. Subsequently, there are two types of estimators [8]:

1. Parameter estimators (static estimation problem); for example, Wiener-Hopf filter
2. State estimators (dynamic estimation problem); for example, KF

B. ESTIMATION TECHNIQUES

The following estimation techniques can be employed if the POI is a random variable:

- maximum a posteriori (MAP) estimator
- minimum mean-square error (MMSE) estimator
- linear minimum mean-square error (LMMSE) estimator

It turns out that the KF is the MMSE state estimator if the initial state and noise entering into the system are Gaussian. In the non-Gaussian case, the KF is still a LMMSE state estimator [10]. To get a good understanding of the KF problem and its solution, some underlying concepts related to KF are discussed next.

C. THE KALMAN FILTER

Let $\underline{x}(k)=[x_{1_x}(k), x_{2_x}(k), \dots, x_{n_x}(k)]^T$ be the state of a discrete-time, linear system and $\underline{u}(k)=[u_{1_u}(k), u_{2_u}(k), \dots, u_{n_u}(k)]^T$ be the deterministic input to that system at time k .

Then the system state at time $k+1$ is given by the state equation

$$\underline{x}(k+1) = F(k)\underline{x}(k) + G(k)\underline{u}(k) + \underline{v}(k) \quad k = 0, 1, \dots, \quad (3.1)$$

where $F(k)$ is the $n_x \times n_x$ state transition matrix, $G(k)$ is the $n_x \times n_u$ input gain matrix, and $\underline{v}(k)$ is a $n_x \times 1$ zero mean white Gaussian process noise, with covariance matrix $E\{\underline{v}(k)\underline{v}(k)'\} = Q(k)$.

If $\underline{z}(k)=[z_{1_z}(k), z_{2_z}(k), \dots, z_{n_z}(k)]^T$ is the measurement vector, then the measurement or output equation is given by

$$\underline{z}(k) = H(k)\underline{x}(k) + \underline{w}(k) \quad k = 1, 2, \dots, \quad (3.2)$$

where, $H(k)$ is the $n_z \times n_x$ measurement matrix and $\underline{w}(k)$ is $n_z \times 1$ zero mean white Gaussian measurement noise with covariance matrix $R(k) = E\{\underline{w}(k)\underline{w}(k)'\}$.

The underlying assumptions of the previous linear dynamic model are:

1. Sampling interval is constant
2. Matrices $F(k)$, $G(k)$ and $H(k)$ and deterministic input $\underline{u}(k)$ are known for all values of k ,
3. The noise terms are zero mean, white, and uncorrelated, which leads to $E\{\underline{v}(k)\underline{v}(j)'\} = 0$ for all values of k, j .

The notation $\hat{x}(k|k)$ represents the estimate of $x(k)$ at time k based on all measurements up to and including $z(k)$. Similarly, $\hat{x}(k+1|k)$ represents the estimate of $x(k+1)$ at time $k+1$ based on all measurements up to and including $z(k)$. This notation is used extensively in the follow-up discussion. The symbols $P_{xx}(k|k)$ and $P_{xx}(k+1|k)$ represent the covariance matrices of state estimation errors at time k and $k+1$, respectively. The KF estimates the state of the system when a new measurement is obtained. Updating the state estimate when a new measurement is taken can be split into two steps, prediction and correction, which are presented next.

1. Prediction

State estimate, state covariance, and measurement, respectively, are predicted to the next measurement time using the following equations:

$$\hat{\underline{x}}(k+1|k) = F(k)\hat{\underline{x}}(k|k) + G(k)\underline{u}(k), \quad (3.3)$$

$$P(k+1|k) = F(k)P(k|k)F(k)' + Q(k), \quad (3.4)$$

and

$$\hat{\underline{z}}(k+1|k) = H(k+1)\hat{\underline{x}}(k+1|k). \quad (3.5)$$

State prediction error and measurement prediction error are given by

$$\tilde{\underline{x}}(k+1|k) = \underline{x}(k+1) - \hat{\underline{x}}(k+1|k) = F(k)\tilde{\underline{x}}(k|k) + \underline{v}(k) \quad (3.6)$$

and

$$\begin{aligned} \tilde{\underline{z}}(k+1|k) &= \underline{z}(k+1) - \hat{\underline{z}}(k+1|k) \\ &= H(k+1)\tilde{\underline{x}}(k+1|k) + \underline{w}(k+1), \end{aligned} \quad (3.7)$$

respectively, where $\tilde{\underline{z}}(k+1|k)$ is called innovation or measurement residual. The measurement prediction (innovation) covariance matrix S is computed as

$$S(k+1) = H(k+1)P(k+1|k)H(k+1)' + R(k+1), \quad (3.8)$$

and the filter gain is

$$W(k+1) = P(k+1|k)H(k+1)'S(k+1)^{-1}. \quad (3.9)$$

2. Correction

The updated state estimate and state covariance at time step $k+1$ are given by the state update equation and covariance update equation, respectively, as [10]:

$$\hat{\underline{x}}(k+1|k+1) = \hat{\underline{x}}(k+1|k) + W(k+1)\tilde{\underline{z}}(k+1|k) \quad (3.10)$$

and

$$\begin{aligned} P(k+1|k+1) &= P(k+1|k) - P(k+1|k)H(k+1)'S(k+1)^{-1}H(k+1)P(k+1|k) \\ &= P(k+1|k) - W(k+1)S(k+1)W(k+1)'. \end{aligned} \quad (3.11)$$

The flow chart of one KF cycle is presented in Figure 11. The state estimation cycle consists of state and measurement prediction (time update) and state update (measurement update). The covariance calculations are independent of the state and measurements and can be performed offline.

The computational requirements of the KF are approximately proportional to n^3 , $n = \max(n_x, n_z)$. In most cases, a steady-state implementation in which the KF parameters (state error covariance matrix and Kalman gain) are kept constant and pre-computed yields satisfactory results with considerable savings in computations.

3. Riccati Equation

The expression for the state covariance matrix P , given in Equation (3.4), can be written as

$$\begin{aligned} P(k+1|k) &= F(k) \{P(k|k-1) - P(k|k-1)H(k)'S(k)H(k)P(k|k-1)\} \times \\ &\quad F(k)' + Q(k). \end{aligned} \quad (3.12)$$

Equation (3.12) is known as the algebraic matrix Riccati equation, and its solution for a LTI system converges to a finite steady-state (finite) covariance matrix if the pair $\{F, H\}$ is completely observable; i.e., the state can be fully determined from the input and

output measurements. The steady-state covariance matrix is the solution of the algebraic matrix Riccati equation, or simply the algebraic Riccati equation, and yields the steady-state gain for the KF, which is given as

$$K = FPH'(HPH' + R)^{-1}. \quad (3.13)$$

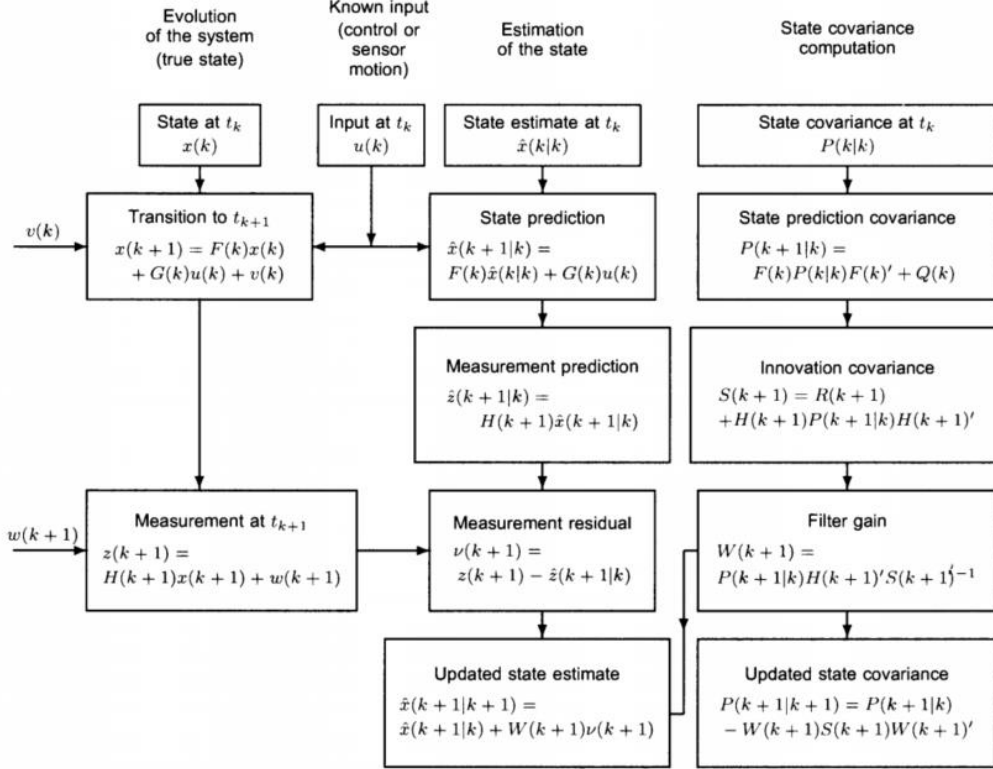


Figure 11. One cycle of KF state estimation, from [8].

D. KALMAN FILTER ESTIMATION OF MULTI-ANTENNA SYSTEMS

Let $x[n]$ be the transmitted DVB-T2 signal and $s[n]$ be the weak signal that is to be recovered. The bandwidth of $s[n]$ is assumed to be much smaller than that of $x[n]$, with a low data rate and longer symbol duration than that of $x[n]$. Such characteristics ensure that the time spread of the two channels is negligible as compared to the symbol duration of $s[n]$, and multipath can be neglected with the two antennas receiving the same copy of $s[n]$.

The signals received at the two antennas are given by

$$y_1[n] = h_1[n] * x[n] + s[n] + w_1[n] \quad (3.14)$$

and

$$y_2[n] = h_2[n] * x[n] + s[n] + w_2[n], \quad (3.15)$$

where $h_1[n]$ and $h_2[n]$ are CIRs that are time-invariant and independent of each other; $w_1[n]$ and $w_2[n]$ are zero mean additive white Gaussian noise at the two antennas with covariance matrices $R = E\{w_1[m]w_1[n]'\}$, and $Q = E\{w_2[m]w_2[n]'\}$. We also assume the noise sequences to be uncorrelated with each other, which leads to $E\{w_1[m]w_2[n]'\} = 0$ for all values of m and n .

Equations (3.14) and (3.15) can also be written, respectively, as

$$y_1[n] = h_{10}[n]x[n] + h_{11}[n]x[n-1] + \dots + h_{1N}[n]x[n-N] + s[n] + w_1[n] \quad (3.16)$$

and

$$y_2[n] = h_{20}[n]x[n] + h_{21}[n]x[n-1] + \dots + h_{2N}[n]x[n-N] + s[n] + w_2[n]. \quad (3.17)$$

Rewriting Equation (3.16), we get

$$x[n] = \frac{1}{h_{10}[n]} \{y_1[n] - h_{11}[n]x[n-1] - \dots - h_{1N}[n]x[n-N] - s[n] - w_1[n]\}. \quad (3.18)$$

Next, Equations (3.18) and (3.17) can be written in matrix form, respectively, as

$$\begin{bmatrix} x[n] \\ x[n-1] \\ \vdots \\ x[n-(N-1)] \end{bmatrix} = \begin{bmatrix} -h_{11}/h_{10} & -h_{12}/h_{10} & \cdots & -h_{1(N-1)}/h_{10} & -h_{1N}/h_{10} \\ 1 & 0 & \cdots & 0 & 0 \\ & & \vdots & & \\ 0 & 0 & \cdots & 1 & 0 \end{bmatrix} \begin{bmatrix} x[n-1] \\ x[n-2] \\ \vdots \\ x[n-N] \end{bmatrix} + \begin{bmatrix} 1/h_{10} \\ 0 \\ \vdots \\ 0 \end{bmatrix} y_1[n] + \begin{bmatrix} -1/h_{10} \\ 0 \\ \vdots \\ 0 \end{bmatrix} [s[n] + w_1[n]] \quad (3.19)$$

and

$$y_2[n] = [h_{21} \ h_{22} \ \cdots \ h_{2N}] \begin{bmatrix} x[n-1] \\ \vdots \\ x[n-N] \end{bmatrix} + [s[n] + w_2[n]], \quad (3.20)$$

where h_{20} has been forced to zero; i.e., $h_2[n]$ is delayed by one time step.

Defining $\underline{x}[n] = \{x[n-1], x[n-2], \dots, x[n-N]\}^T$, we can write Equations (3.19) and (3.20), respectively, in state space form as

$$\underline{x}[n+1] = A\underline{x}[n] + By_1[n] + G\{s[n] + w_1[n]\} \quad (3.21)$$

and

$$y_2[n] = C^T \underline{x}[n] + \{s[n] + w_2[n]\}, \quad (3.22)$$

where the matrices A, B, G and C are defined, respectively, as

$$A = \begin{bmatrix} -h_{11}/h_{10} & -h_{12}/h_{10} & \cdots & -h_{1(N-1)}/h_{10} & -h_{1N}/h_{10} \\ 1 & 0 & \cdots & 0 & 0 \\ & & \ddots & & \\ 0 & 0 & \cdots & 1 & 0 \end{bmatrix} \quad (3.23)$$

and

$$B = \begin{bmatrix} 1/h_{10} \\ 0 \\ \vdots \\ 0 \end{bmatrix}, \quad G = \begin{bmatrix} -1/h_{10} \\ 0 \\ \vdots \\ 0 \end{bmatrix}, \quad C = \begin{bmatrix} h_{20} \\ h_{21} \\ \vdots \\ h_{2N} \end{bmatrix}. \quad (3.24)$$

Equations (3.21) and (3.22) yield the state-space model which was described by Equations (3.1) and (3.2). The recursive estimate of the state $\underline{x}[n]$ can be computed by the KF, where the received sequence $y_1[n]$ is the known KF input and the received sequence $y_2[n]$ is the measurement.

Since neither CIRs change over time, the matrices A, B, C and G are constant. Writing Equations (3.10) and (3.11) according to the state-space model of Equations (3.21) and (3.22), we get

$$\hat{\underline{x}}[n+1] = A\hat{\underline{x}}[n] + By_1[n] + K[n]\{y_2[n] - C\hat{\underline{x}}[n]\}. \quad (3.25)$$

At this point, Equation (3.23) can be rewritten in the following form

$$\hat{\underline{x}}[n+1] - \{A - KC\} \hat{\underline{x}}[n] = By_1[n] + Ky_2[n], \quad (3.26)$$

where K is the KF gain in steady-state and is given by Equation (3.13). Rewriting Equation (3.24) in the z-domain leads to

$$\hat{\underline{X}}(z) = \left[\{zI - (K - AC)\}^{-1} B \right] Y_1(z) + \left[\{zI - (K - AC)\}^{-1} K \right] Y_2(z), \quad (3.27)$$

where $\hat{\underline{X}}(z) = [z^{-1}X(z), z^{-2}X(z), \dots, z^{-N}X(z)]^T$ is the z-transform of the sequence $\hat{\underline{x}}[n] = \{\hat{x}[n-1], \hat{x}[n-2], \dots, \hat{x}[n-N]\}^T$.

It can be shown that for $\hat{\underline{x}}[n] = \{\hat{x}[n-1], \hat{x}[n-2], \dots, \hat{x}[n-N]\}^T$, $\hat{x}[n-1] = [1 \ 0 \ 0 \dots] \hat{\underline{x}}[n]$, $\hat{x}[n-2] = [0 \ 1 \ 0 \dots] \hat{\underline{x}}[n]$ and so on; therefore, estimates of states at time $n-1$ and time $n-2$ are given, respectively, by

$$\begin{aligned} z^{-1} \hat{\underline{X}}(z) &= [1 \ 0 \ 0 \dots] \left[\{zI - (K - AC)\}^{-1} B \right] Y_1(z) + \\ &\quad [1 \ 0 \ 0 \dots] \left[\{zI - (K - AC)\}^{-1} K \right] Y_2(z) \end{aligned} \quad (3.28)$$

and

$$\begin{aligned} z^{-2} \hat{\underline{X}}(z) &= [0 \ 1 \ 0 \dots] \left[\{zI - (K - AC)\}^{-1} B \right] Y_1(z) + \\ &\quad [0 \ 1 \ 0 \dots] \left[\{zI - (K - AC)\}^{-1} K \right] Y_2(z). \end{aligned} \quad (3.29)$$

Similarly, estimates of states at other time steps can be found using the logic described before.

From Equations (3.26) and (3.27), it can be concluded that two transfer functions are needed to produce the estimate of transmitted data at different discrete times when applied to the received sequences $y_1[n]$ and $y_2[n]$; thus, estimating the state $\hat{x}[n-1]$ requires two transfer functions

$$G_1(z) = [1 \ 0 \ 0 \dots] \left[\{zI - (K - AC)\}^{-1} B \right] \quad (3.30)$$

and

$$G_2(z) = [1 \ 0 \ 0 \dots] \left[\{zI - (K - AC)\}^{-1} K \right]. \quad (3.31)$$

The aforementioned transfer functions have the form

$$G_1(z) = \frac{J_1(z)}{V(z)}, \quad G_2(z) = \frac{J_2(z)}{V(z)}. \quad (3.32)$$

Equation (3.27), thus, takes the form

$$z^{-1}X(z) = \frac{J_1(z)}{V(z)}Y_1(z) + \frac{J_2(z)}{V(z)}Y_2(z) \quad (3.33)$$

or

$$z^{-1}X(z)V(z) = J_1(z)Y_1(z) + J_2(z)Y_2(z). \quad (3.34)$$

Equation (3.32) can be expressed in the time-domain as

$$\hat{x}[n-1] * v[n] = J_1[n] * y_1[n] + J_2[n] * y_2[n]. \quad (3.35)$$

Equation (3.33) can also be written as

$$\begin{aligned} \hat{x}[n-1] &= J_1[1]y_1[n] + J_1[2]y_1[n-1] + \dots \\ &\quad + J_2[1]y_2[n] + J_2[2]y_2[n-1] + \dots \\ &\quad - v[1]\hat{x}[n-2] - v[2]\hat{x}[n-3] - \dots \end{aligned} \quad (3.36)$$

In matrix form, we can write Equation (3.34) as

$$\begin{aligned} \hat{x}[n-1] &= [J_1[1] \ J_1[2] \dots] \begin{bmatrix} y_1[n] \\ y_1[n-1] \\ \vdots \end{bmatrix} + [J_2[1] \ J_2[2] \dots] \begin{bmatrix} y_2[n] \\ y_2[n-1] \\ \vdots \end{bmatrix} + \\ &\quad [-v[1] \ -v[2] \dots] \begin{bmatrix} \hat{x}[n-2] \\ \hat{x}[n-3] \\ \vdots \end{bmatrix}. \end{aligned} \quad (3.37)$$

Equation (3.35) is implemented to estimate the state of the transmitted DVB-T2 signal. The Kalman gain parameter is calculated using the MATLAB function 'dlqe.m', while coefficients of the two transfer functions are calculated using the MATLAB function 'ss2tf.m' function. These transfer functions are implemented using two discrete time filters, and received sequences are then passed through these two filters. Next, the

outputs are combined to provide the DVB-T2 signal estimate. This process is illustrated in Figure 12. Note that Kalman gain and coefficients of the transfer functions are calculated offline at the beginning of the simulation and then updated only periodically.

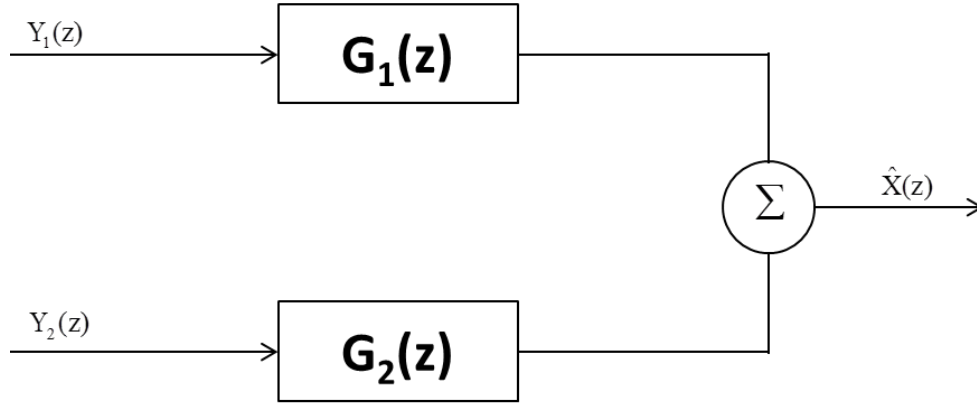


Figure 12. Transfer function approach to estimate state of transmitted data.

In this chapter, we discussed the KF based approach designed to use the two estimated CIRs and signals received at the antenna to estimate the state of the strong interferer DVB-T2 signal. Specifically, we showed that we can obtain the estimate of the signal received at the second antenna by using the estimated DVB-T2 signal and estimated CIR of the second channel. Subtraction of estimated signal from the original signal received at second antenna suppresses the interference, which allows the recovery of the weak signal. This approach was implemented in Simulink, and simulation results are discussed in Chapter IV.

IV. SIMULATION AND RESULTS

Theoretical background to recover a weak signal in the presence of a strong co-channel interferer was presented in preceding chapters. Simulink models were developed to evaluate the robustness of the proposed approach to noise distortions. In this chapter, we first present the scheme implemented. Next, we introduce concepts of SNR and SIR. Finally, we investigate the approach robustness to SNR, SIR, and estimated CIR accuracy.

As mentioned earlier, the received signal at each antenna consists of a strong DVB-T2 signal (after passing through a channel), a weak signal-of-interest and additive white Gaussian noise. In this study, the weak signal s is a narrow-band signal modulated to a carrier and is embedded in interference and noise as shown in Figure 13.

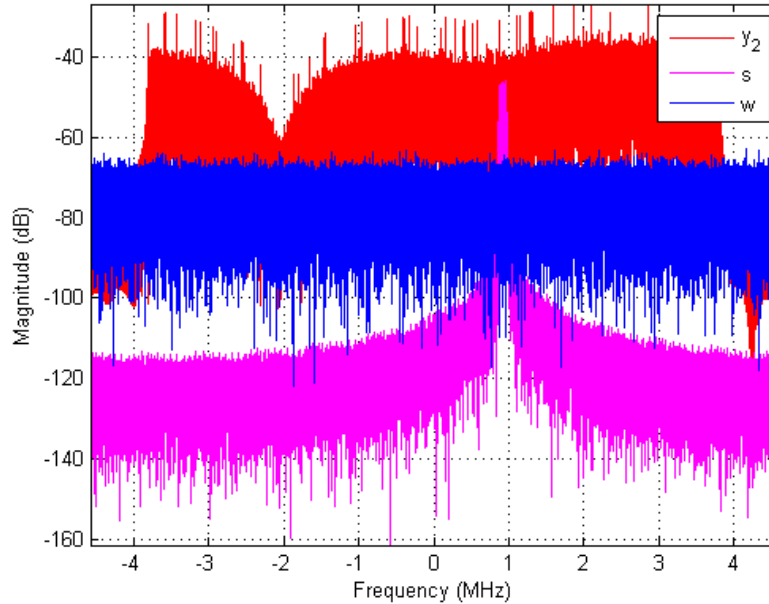


Figure 13. Frequency domain plot of interferer (y_2), weak signal (s) and noise (w) for SNR=20 dB and SIR= -25 dB.

It has been shown theoretically that the state of a signal can be estimated using the KF framework described in Chapter III. The said framework is used to estimate the

transmitted DVB-T2 sequence, which requires knowledge of CIRs. Pilots present in the DVB-T2 signal are used to estimate both CIRs. Convolution of the estimated DVB-T2 sequence with one of the estimated CIR provides us with an estimate of the signal received at the antenna corresponding to that channel. The subtraction of the estimated TV broadcast signal from the overall signal received at the antenna is designed to remove the contribution of the strong TV broadcast signal and preserve the weak signal and noise, from which the weak signal can be extracted. This scheme is presented in Figure 14.

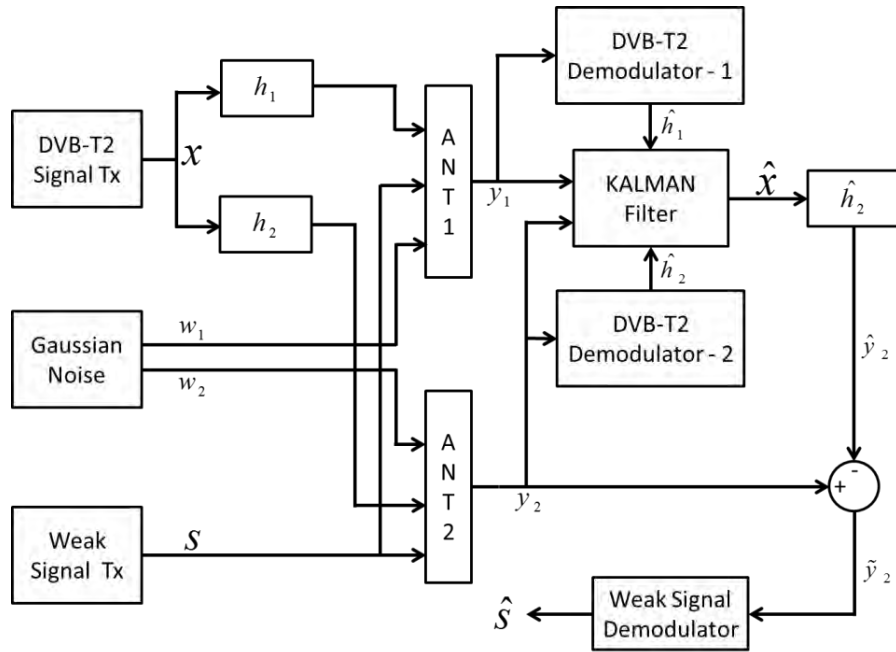


Figure 14. Block diagram for recovering weak signal.

As evident from the above scheme, the strong interferer contribution can be minimized, as shown in Figure 15, provided accurate estimates of \hat{x} , \hat{h}_1 and \hat{h}_2 are obtained. The resulting signal is a combination of the weak signal and noise which then becomes a standard demodulation problem, and the weak signal can be recovered easily, as illustrated in Figure 16.

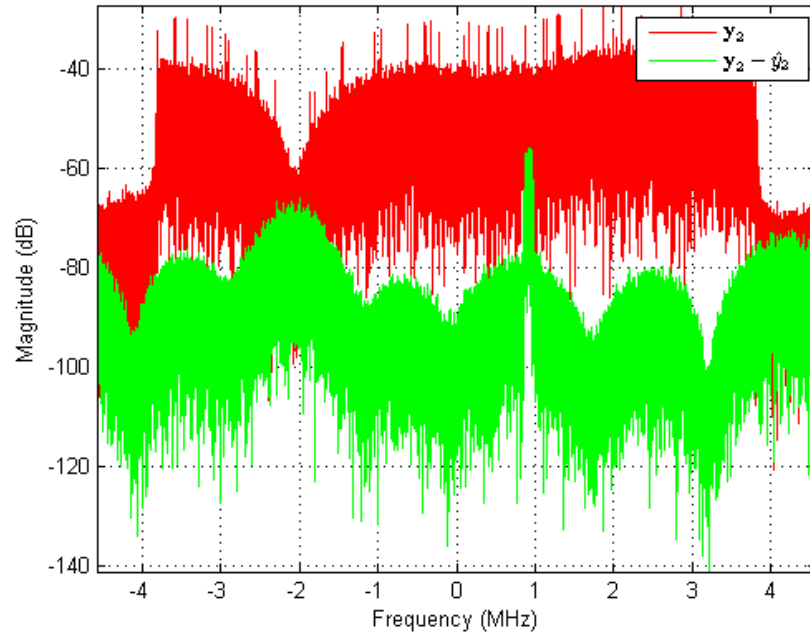


Figure 15. Suppression of interference and recovery of weak signal for SNR=20 dB and SIR= − 25 dB.

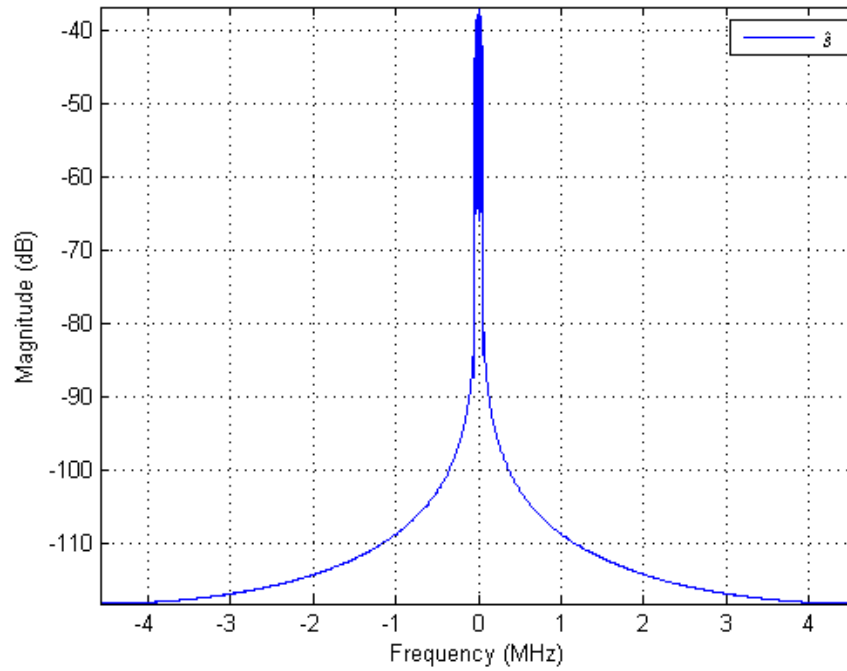


Figure 16. Recovered weak signal (\hat{s}) after demodulation for SNR=20 dB and SIR= − 25 dB.

A. SIMULINK IMPLEMENTATION

The scheme shown in Figure 14 was implemented in Simulink, using x and s as zero mean QPSK signals. The signal x is implemented at baseband, while s is band limited by a square root-raised cosine filter and modulated at a carrier frequency equal to 914.286 kHz. Since both x and s are complex signals, zero-mean independent, complex white Gaussian noise w_1 and w_2 are added at both antennas.

For simplicity, no coding was applied and perfect synchronization both in time and frequency was assumed. The results presented further in the research were obtained by running the simulation for 10^7 symbols of the weak signal. Performances are evaluated in terms of bit error ratio (BER) of both DVB-T2 and weak signals at different SNRs and SIRs.

1. Signal-to-Noise Ratio and Signal-to-Interference Ratio

Recall that two sources of disturbances are present: the TV broadcast interference and the AWGN. Thus, two power level ratio quantities relative to the signal-of-interest are the signal-to-interference ratio and the signal-to-noise ratio, respectively, defined as

$$SIR = \frac{\sigma_s^2}{\sigma_x^2} \text{ and } SIR_{dB} = 20 \log_{10} \left(\frac{\sigma_s}{\sigma_x} \right), \quad (4.1)$$

where σ^2 and σ represent variance and standard deviation, respectively, and x is normalized to 1, which means $\sigma_x^2 = \sigma_x = 1$. Thus, for a given SIR, σ_s is given by

$$\sigma_s = 10^{\frac{SIR}{20}}. \quad (4.2)$$

Since s is band limited with bandwidth equal to 91.2 kHz and the noise is white, the term SNR can be defined as

$$\begin{aligned} SNR_{dB} &= 20 \log_{10} \left(\frac{\sigma_s}{B_s N_w} \right) \\ &= 20 \log_{10} \left(\frac{\sigma_s}{\sigma_w} \right) + 20 \log_{10} \left(\frac{B_w}{B_s} \right), \end{aligned} \quad (4.3)$$

where N_w is the two-sided noise power spectral density, and B_s and B_w represent the bandwidths of weak signal s and white noise w , respectively. For a given SNR and σ_s , σ_w can be obtained from Equation 4.2 as

$$\sigma_w = \sigma_s 10^{\frac{SNR - 20 \log_{10}(B_w/B_s)}{20}}. \quad (4.4)$$

Note that both CIRs are normalized, meaning the power of the signals passing through the channels remains the same. Since $\sigma_x^2 = \sigma_x = 1$, the signals y_1 and y_2 received at the antennas also have variances $\sigma_{y_1}^2 = \sigma_{y_2}^2 = 1$. Therefore, the preceding definitions of SNR and SIR also hold for signals y_1 and y_2 . For simulation purposes, we first defined SIR and SNR and set standard deviations for s and w to achieve the desired SIR and SNR.

2. Estimated CIR

Recall that DVB-T2 pilots are used to estimate the CIRs for equalization in DVB-T2 receiver and to estimate the state, as shown earlier in Figure 14. Simulation results showed that BER of 10^{-3} and below were achieved for the estimated DVB-T2 signal using estimated CIRs; however, the same type of performance was not observed for the weak signal BER when the estimated CIR parameters were used in the KF step for the DVB-T2 signal state estimation. In this case, the best BER achieved for the weak signal was equal to 0.15; hence, results show that estimating the CIR characteristics using the pilots' information is sufficient for DVB-T2 signal demodulation but is not for the weak signal demodulation process. Therefore, original CIRs coefficients and variants with 5%, 10%, and 15% random errors in coefficient values were used as estimated CIRs in the simulations to evaluate the sensitivity of the overall proposed scheme to degradations in estimated CIR characteristics.

Results showed that the estimation process breaks down when CIR estimates have a 20% error. At that point, both estimated CIRs carry the same information, and the independence condition of the two channels needed for the scheme to work breaks down.

In turns, the KF implementation becomes ill-conditioned and is unable to predict the state of the DVB-T2 signal.

B. SIMULATION RESULTS

The simulation scheme mentioned above was implemented in Simulink. The results obtained are discussed below.

1. Signal Attenuation

As noted above, recovering the weak signal is possible only when the transmission channels associated with the two-antenna receiver are independent, in the sense that their associated transfer functions have different root locations, ensuring the combined state space system is fully observable and controllable.

We investigated the effectiveness of this system by observing the attenuations of the two received broadcast signals y_1 and y_2 , the signal-of-interest s and, finally, the noise w . Since the parameters at the receiver are adjusted on the basis of the estimated multipath of the TV broadcast signal, sensitivity of these parameters to errors in the channel estimates is also inspected.

Recall that the broadcast TV signals y_1 and y_2 , received through the multipath channels, need to be highly attenuated with respect to the signal-of-interest s while the noise w is not amplified by the receiver for the proposed scheme to be successful. Thus, we tested the receiver ability to separately attenuate signals y_1 , y_2 , s , and w by broadcasting the following signal combinations:

- DVB-T2 signals y_1 and y_2 only
- noise w only
- signal- of-interest s only

In each case, we computed the power attenuation (or gain) level in dB between each test signal (y_1 and y_2, s, w) as input and the resulting output ($\tilde{y}_2 = y_2 - \hat{y}_2$). The attenuation parameter is defined as

$$Attn_x(dB) = 10 \log_{10} \frac{\sigma_x^2}{\sigma_{\hat{y}_2}^2}, \quad (4.5)$$

where σ_x^2 represents the variance of the signal whose attenuation level is to be observed.

a. Interference Attenuation

First we apply the broadcast TV signals y_1 and y_2 as inputs, without noise w or signal-of-interest s present. Attenuation levels for signals y_1 and y_2 obtained with actual CIRs and with 5%, 10 %, 15% error levels for estimated CIRs are plotted in Figure 17 and Figure 18, respectively. Results show that when actual CIRs are used as estimated CIRs, signals y_1 and y_2 are completely suppressed. The level of attenuation obtained for signals y_1 and y_2 increases with the level of accuracy in the estimated CIR parameters. It can also be observed that the attenuation level is insensitive to noise power changes.

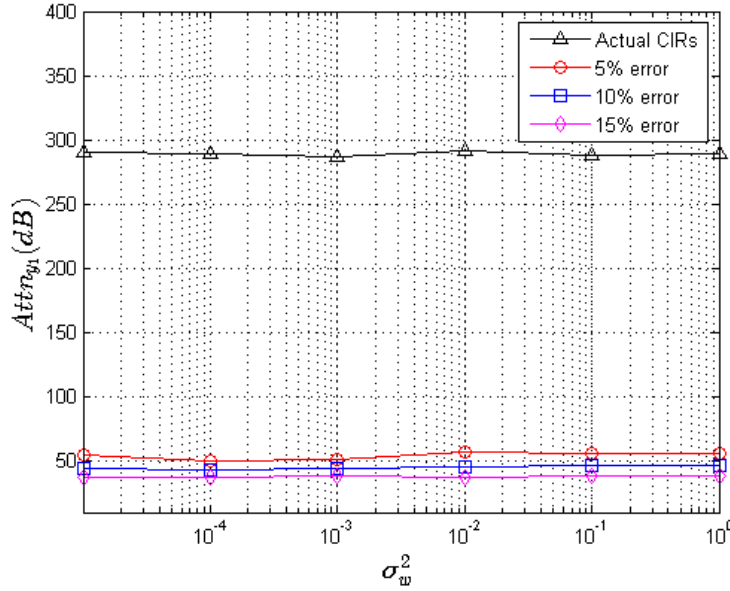


Figure 17. Attenuation of the interference y_1 for different noise power levels and error percentages in the estimated CIR coefficients.

It is worth noting that the KF becomes deterministic when exact CIR parameters are known and no other disturbance (noise w or signal-of-interest s) is present;

therefore, the innovation of the KF is equal to zero in steady-state. Since this case represents a deterministic observer, the state estimation error in steady-state is equal to zero, which leads to infinite attenuation.

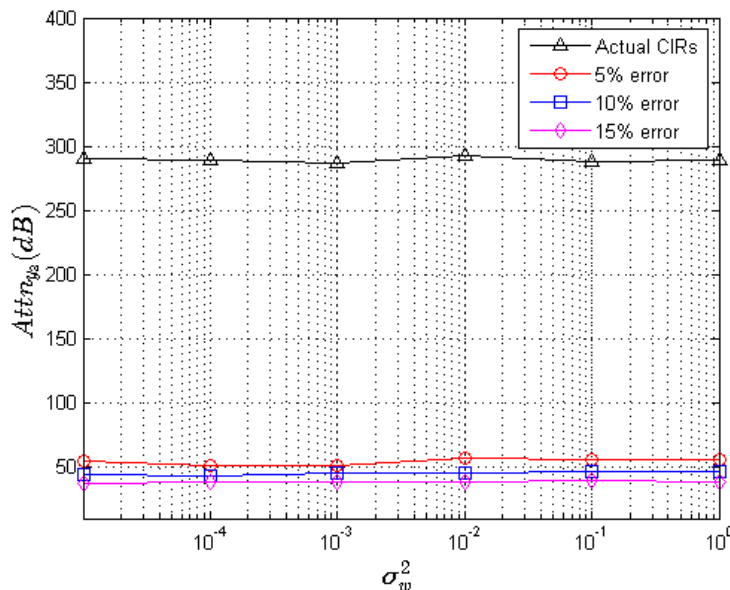


Figure 18. Attenuation of the interference y_2 for different noise power levels and error percentages in the estimated CIR coefficients.

Any other CIR parameter error yields nonzero attenuation for signals y_1 and y_2 . Due to the optimality of the KF, the sensitivity to errors in the estimated CIR parameters is minimized, which is indicated by a high attenuation (about 50 dB) for the range of noise variance levels considered in this implementation.

b. Signal of Interest Attenuation

In the second case, we apply the signal-of-interest s as input without broadcast TV signals y_1 and y_2 or noise w present. Attenuation levels for s obtained with actual CIRs and with 5%, 10 %, and 15% error levels for estimated CIRs are plotted in Figure 19. It can be seen from Figure 19 that s is attenuated by approximately 9.5 to 10 dB, and the level of attenuation observed for s is independent of noise power level variations in the KF.

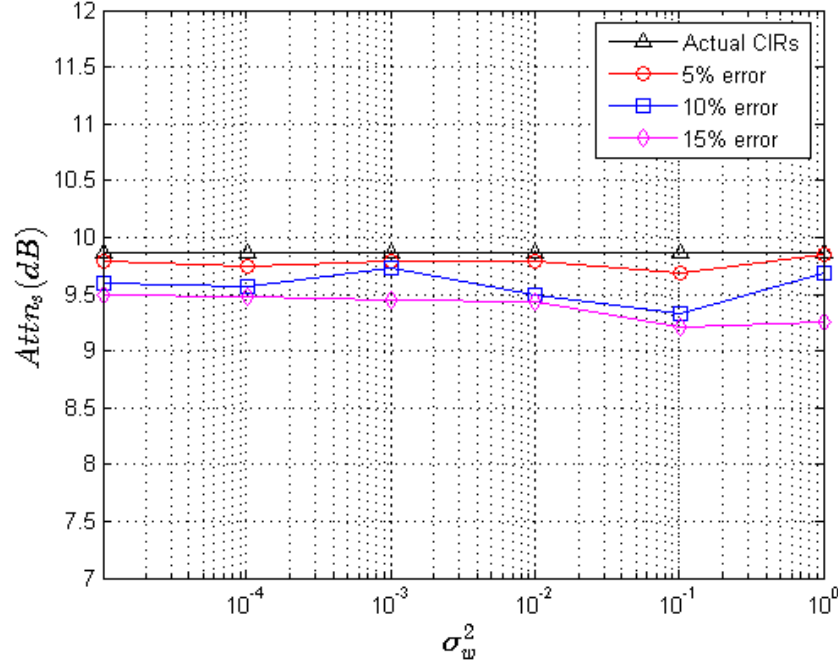


Figure 19. Attenuation of the signal s for different noise power levels and error percentages in the estimated CIR coefficients.

c. Noise Attenuation

In the third case, we apply the noise w as input without broadcast TV signals y_1 and y_2 or signal-of-interest s present. Attenuation levels for w obtained with actual CIRs and with 5%, 10 %, and 15% error levels for estimated CIRs are plotted in Figure 20. Results show the noise w attenuation is about 10 to 10.5 dB. Again, the attenuation level does not change significantly with noise power levels variations.

It has been shown that y_1 and y_2 suffer far more attenuation than that experienced by s , w_1 and w_2 ; hence, \tilde{y}_2 consists of predominantly the weak signal s and the noise w and only includes a negligible contribution from the signal y_2 .

A basic requirement of the system considered is that the signal-of-interest has low power so that it does not interfere with TV broadcasting demodulation. Having established that the scheme presented in the research suppresses the interference in all noise conditions, we now evaluate its performance by calculating BER for the DVB-T2

and the weak signal at different SIRs and SNRs. Our goal is to identify some SIR and SNR where BER is less than 10^{-3} in order to correctly demodulate both the interference and the weak signal. For this reason, BER is plotted against SNR at different SIRs for the DVB-T2 signals, received from two different channels, and the weak signal.

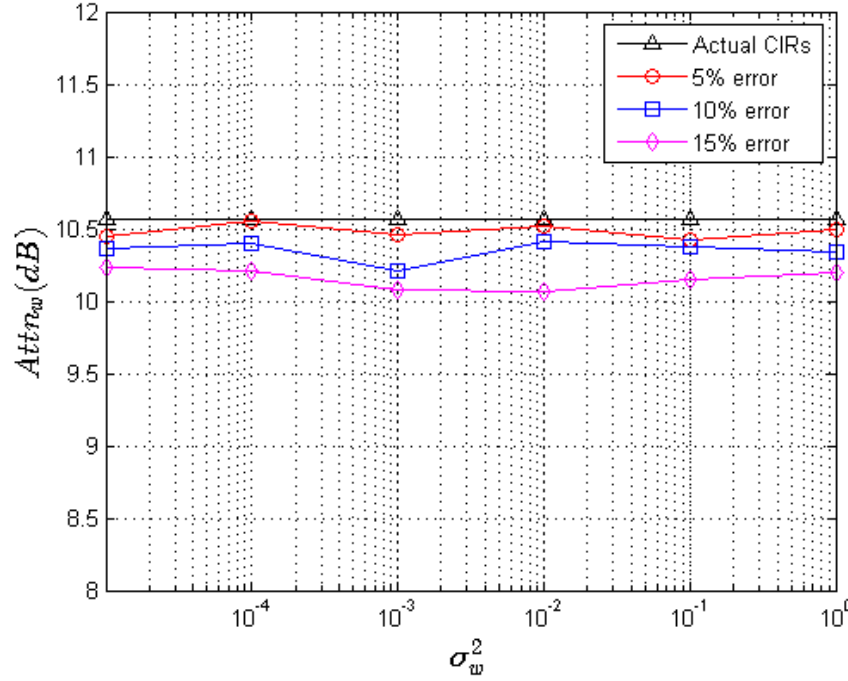


Figure 20. Attenuation of the noise w for different noise power levels and error percentages in the estimated CIR coefficients.

2. DVB-T2 BER Performance Analysis

It is evident, as expected, from Figure 21 and Figure 22 that the BER obtained for the DVB-T2 signal decreases with smaller SIR.

For the signal transmitted through channel 1, a BER below 10^{-3} was obtained with SNR=10 dB and SIR=-25 dB. However, for the signal transmitted through channel 2, a BER of less than 10^{-3} was achieved with SNR=25 dB and SIR=-25 dB. Hence, these results show that the BER for the DVB-T2 signal depends on the noise level present in the channel. Some type of signal processing should be considered to select the signal from the channel which has the lower BER.

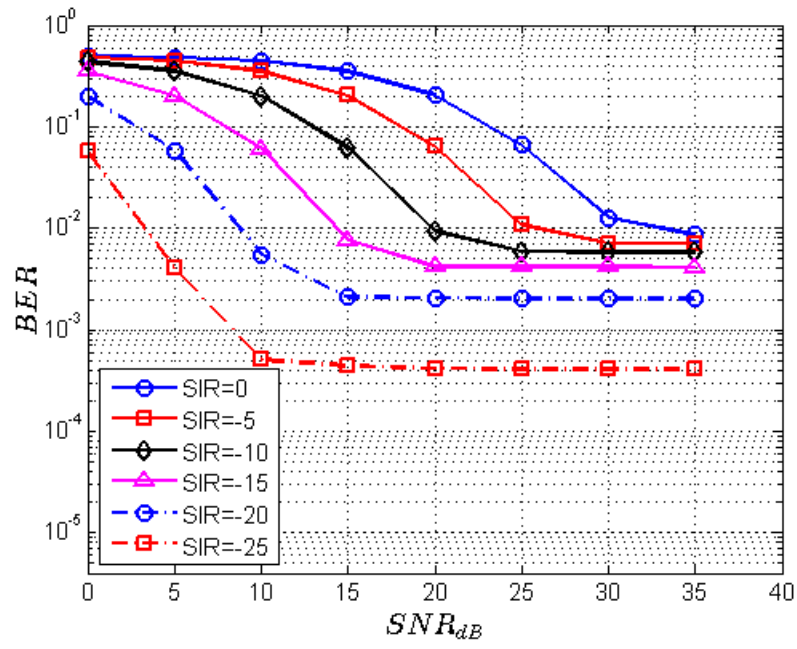


Figure 21. DVB-T2 Channel 1 signal BER at different SIR.

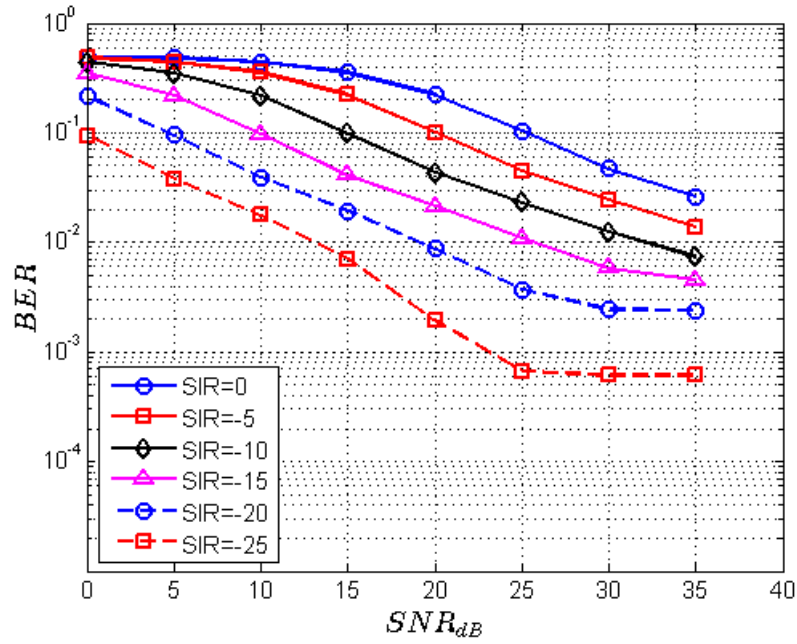


Figure 22. DVB-T2 Channel 2 signal BER at different SIR.

3. Weak Signal BER Performance Analysis

Due to the high attenuation of TV interference in the proposed system, the contribution of the TV component in the resulting signal ($\tilde{y}_2 = y_2 - \hat{y}_2$) is smaller than that of the signal-of-interest and noise. Consequently, results show that the BER for the weak signal is not affected by variations in the TV signal power and, therefore, BER remains constant for all SIR considered.

It was shown earlier that the attenuation level of the broadcast TV interference increases as estimated CIRs coefficients accuracy improves; however, this had no bearing on the BER of the weak signal. Results indicated that with 0 to 15% errors in the estimated CIR coefficients, the BER obtained for the weak signal remained constant. When estimated CIR coefficients have 20% or more error, the KF estimation process breaks down, and the weak signal cannot be recovered.

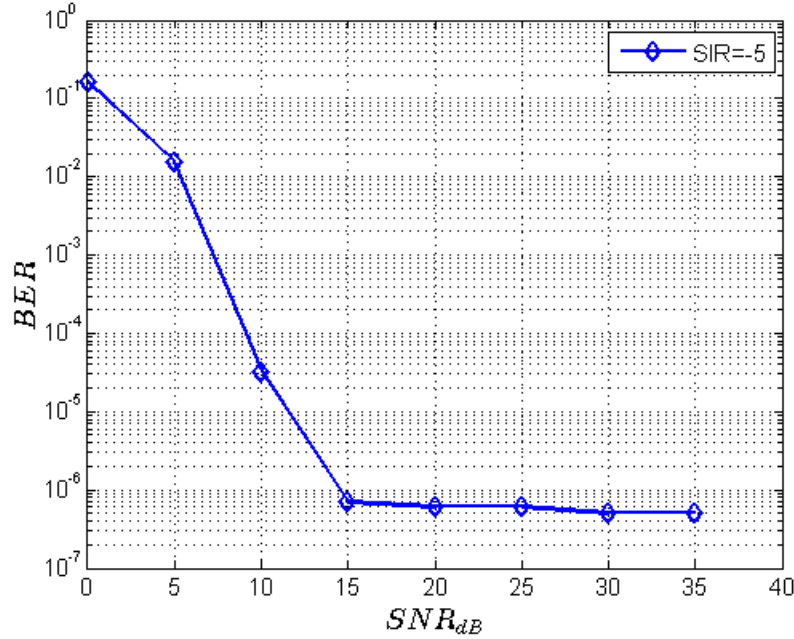


Figure 23. Weak signal BER with SIR = -5 dB and 15% error in estimated CIR coefficients.

Simulations showed that the BER obtained for the weak signal remain constant irrespective of the SIR or when estimated CIRs have 0 to 15 percent errors in their

coefficients. Therefore, only BER obtained for the weak signal with $\text{SIR} = -5 \text{ dB}$ and 15% error level in estimated CIRs coefficients are presented in Figure 23. It is observed from Figure 23 that a minimum SNR equal to 7dB is required to ensure a maximum BER of 10^{-3} . Similar results were obtained at different SIRs and with different error percentages in the estimated CIR coefficients.

Overall results indicate that the proposed scheme can be used to recover the weak signal-of-interest from the co-channel interference signal without distorting the interference signal provided estimated CIRs have 15 percent or less errors in their coefficients and the SIR is below -25 dB . Results are summarized in Chapter V, and our conclusions and recommendations for future work are presented.

THIS PAGE INTENTIONALLY LEFT BLANK

V. CONCLUSIONS AND RECOMMENDATIONS

The purpose of this thesis was to recover a weak signal in the presence of a strong interference signal and noise. The interference signal was assumed to be affected by multipath and the two paths present to be independent of each other. The interference component was modeled as a DVB-T2 signal at baseband, while the weak signal was selected as a narrowband carrier modulated QPSK signal not affected by multipath.

A two-antenna model using KF was presented to estimate the state of the interference signal using channel diversity at the receiver. The known overhead in the TV broadcast interference signal was used to estimate the transmission Channel Impulse Responses (CIRs) that are used to equalize the TV broadcast signal with the resulting BER below 10^{-3} for the DVB-T2 signal. However, a BER of 10^{-3} or below for the estimated weak signal could not be obtained as the channel estimation scheme based using only the DVB-T2 pilots information was not accurate enough. Therefore, the research conducted in this study assumes that the transmission channel estimation can be done accurately and investigates the robustness of the proposed scheme to estimated CIR coefficients level of accuracy.

The proposed KF demodulation is based on the CIRs, and the approach is shown to be effective in the presence of some level (up to 15%) of errors in the CIR estimates. Results also show that the approach breaks down when CIR estimates have 20% or more error. At that point, both estimated CIRs carry the same information, and the requisite independence condition between the two channels no longer holds true. The KF implementation becomes ill-conditioned and is unable to predict the state of the DVB-T2 signal.

Results also show that significant TV broadcast interference attenuation is obtained when using actual or estimated CIRs in the KF operation. In such cases, the signal obtained afterwards is mostly composed of the weak signal and noise, out of which the weak signal can be easily recovered. Results obtained indicate that interference BER

improves with decreasing SIR. In addition, it has also been observed that the weak signal BER is independent of the SIR and is a function of SNR alone.

Follow-on research should include a more robust approach for estimating the channel coefficients so that it can be seamlessly integrated into the existing model.

APPENDIX. MATLAB CODE

Matlab code used in the research along with associated functions is given below.

1. Main File

```
clc
clear all
close all
%% Load Model

model = 'KalmanOne_h1h2_Actual_Latest_SNR';
load_system(model)

stop_weak = 1e3;
stop_int = inf;
rho = 0/100;
iter = 100;

%% Transmission channel parameters

h1=[0.7+0.3i, 2.3-.1i, -0.9+0.4i, 0.2i];
h2=[0.3+0.9i, 0.1-0.4i, -1.3i, 2.2+.02i];

h1 = [h1,zeros(1,10-length(h1))];
h2 = [h2,zeros(1,10-length(h2))];

h1 = h1 / sqrt(h1*h1');
h2 = h2 / sqrt(h2*h2');

Up = 100; %Up sampling & down sampling rate for weak
signal

% Frequencies
Fs=(64/7)*1e06; % sampling and symbol
rate for DVB-T2 signal
M=4; % M-QAM
M_weak = 4; % M-PSK
ph_weak = pi/4; % phase-offset
Fb=log2(M)*(1512/(2048+64))*Fs; % bit rate for DVB-T2 signal

% Weak Comms Signal

Fc=Fs/10; % carrier frequency for weak signal
Fdw=Fc/10; % data rate for weak signal

%% DVB-T Settings

% DVB-T settings:
% Kdata = data subcarriers (68x1512)
```

```

% Kpilots = pilots subcarriers (68x176)
% Ktps = TPS subcarriers (68x17)
% 1512+176+17=1705
% nulls=2048-1705=343

[Kmod, Kdem, Kdata, Xoh, Koh, Nk,NFFT, NCP]=dvbtf2k;
Kpilots=Koh(:, 1:Nk(2));
Xpilots=Xoh(:, 1:Nk(2));
[KH, XpH, IK, Minv]=channelestimator(Kpilots, Xpilots,NFFT);

%noise variance (account for BOOST pilot)
Ps = 1; %signal power=unity power=OFDM
data power
L = NFFT/32; %prefix length(420)
Ndata = 1512;
Ntps = 17;
Npilot = 176;
N = NFFT; %OFDM data length(2112)
r_pilot = 16/9; %pilot power boost factor
G = 1 + (L/(Ndata+Ntps+Npilot*r_pilot));
%eps_noise = Ps*G/(log2(M)*SDnoise^2); %noise power(assume
zero-mean)

%compute the normalize gain factor K(account for BOOST pilot)
N = NFFT;
Ndata = 1512;
Npilot = 176;
Ntps = 17;
K = N/sqrt(Ndata+Npilot*r_pilot+Ntps); %gain factor to
normalize total power

%% Ratios
%
SNRdB = [-20,-15,-10,-5,0,5,10];
SIRdB =-25*(ones(size(SNRdB)));

Attn = 1/10; % Attenuation for received signal
Rx_gain = 1e2; % Gain for shat

SDint = 1;
SDsig_array = (10.^(SIRdB./20)).*SDint;
SDnoise_array =(10.^-((SNRdB+20)./20)).*SDsig_array;

for j = 1 : length(SNRdB)
    SDsig = SDsig_array(:,j);
    SDnoise = SDnoise_array(:,j);
    eps_noise = Ps*G/(log2(M)*SDnoise^2); %noise power(assume
zero-mean)
    for i = 1:iter
        h1est_array(i,:)=h1+rho*h1.*(randn(size(h1))+sqrt(-
1)*randn(size(h1)))/sqrt(2);
        h2est_array(i,:)=h2+rho*h2.*(randn(size(h2))+sqrt(-
1)*randn(size(h2)))/sqrt(2);
    end
end

```

```

        [num1_array(i,:),num2_array(i,:),den_array(i,:)] =
kalmaninitial (hlest_array(i,:),h2est_array(i,:),SDnoise);
    end
    hlest = sum(hlest_array)/iter;
    h2est = sum(h2est_array)/iter;
    num1 = sum(num1_array)/iter;
    num2 = sum(num2_array)/iter;
    den = sum(den_array)/iter;

    sim(model)

    SNR(j,:) = 10*log10 (var(s)/var(w))+20;
    SIR(j,:) = 10*log10(var(s)) / ((var(y1)+var(y2))/2);
    Pb_weak(j,:) = err_weak(end,1);
    Pb_int1(j,:) = err_int1(end,1);
    Pb_int2(j,:) = err_int2(end,1);
    toterr_weak(:,j) = err_weak(size(err_weak,1)-1e1:end,2);
    toterr_int1(:,j) = err_int1(size(err_int1,1)-1e1:end,2);
    toterr_int2(:,j) = err_int2(size(err_int2,1)-1e1:end,2);

end
RHO = rho.*ones(size(SNR));
result = [RHO,SNR,SIR,Pb_int1,Pb_int2,Pb_weak];
str = 'Simulation complited on PC-2';
email(str);

```

2. DVB-T2 FRAME (courtesy Prof. Cristi)

```

function [Kmod, Kdem, Kdata, Xoh, Koh, Nk,NFFT, NCP]=dvbtframe2k
% [Kmod, Kdem, Kdata, Xoh, Koh, Nk,NFFT, NCP]=dvbtframe2k
% where
%
% Kdata = data FFT indices for each OFDM frame ("one" based),
68x1512
% Kmod = overhead FFT indices for each OFDM frame ("one" based),
68x536
%      with Kmod=[Kdata, Kpilots, Ktps, Knulls] of dimensions 68
x 1512, 176, 17, 343
% Xoh = transmitted values of each overhead subcarriers, 68x536
%      with Xoh=[Xpilots, Xtps, Xnulls] of deimensions 68 x
176, 17, 343
% Kdem = map FFT subcarriers back to [data, pilots, tps, nulls]
vector
% Nk=[Ndata, Npilots, Ntps, Nnulls]

%%%%%%%%%%%%%%%%%%%%%%%%%%%%%%%%%%%%%%%%%%%%%%%%%%%%%%%%%%%%%%%%%%%%%%%%%%%%%%
%%%%%%%%%%%%%%%%%%%%%%%%%%%%%%%%%%%%%%%%%%%%%%%%%%%%%%%%%%%%%%%%%%%%%%%%%%%%%%
% From the DVB-T Standard (just choose one mode for simplicity)
% 2k MODE PARAMETERS:
NFFT=2048;

```

```

NCP=NFFT/32; % length of Guard Interval (or Cyclic Prefix)
Kmin=0; Kmax=1704;
Ndata=1512; % data subcarriers
Npilots=176; % pilots subcarriers;
Nnulls=343; % nulls subcarriers
Ntps=17; % Transmission Parameter Signalling (TPS)
subcarriers
Nk=[Ndata, Npilots, Ntps, Nnulls];

% CELLS ALLOCATION:
% Continual Pilots Cells
kcp=[0, 48, 54, 87, 141, 156, 192, ...
     201, 255, 279, 282, 333, 432, 450, ...
     483, 525, 531, 618, 636, 714, 759, ...
     765, 780, 804, 873, 888, 918, 939, ...
     942, 969, 984, 1050, 1101, 1107, 1110, ...
     1137, 1140, 1146, 1206, 1269, 1323, 1377, ...
     1491, 1683, 1704];
% Scattered Pilots Cells
Ksp(1:4:68,:)=ones(17,1)*(3*0+12*(1:142)); % ell mod 4 =0
Ksp(2:4:68,:)=ones(17,1)*(3*1+12*(0:141)); % ell mod 4 =1
Ksp(3:4:68,:)=ones(17,1)*(3*2+12*(0:141)); % ell mod 4 =2
Ksp(4:4:68,:)=ones(17,1)*(3*3+12*(0:141)); % ell mod 4 =3

% TPS (Transmission Parameters Signalling) Cells
ktps=[34, 50, 209, 346, 413, ...
      569, 595, 688, 790, 901,...
      1073, 1219, 1262, 1286, 1469, ...
      1594, 1687];

% Pseudoandom BPSK values for pilots, depnding on subcarriers
only)
% (for simplicity just put random values):
Xp=(4/3)*sign(randn(1,NFFT)); % same form as the DVB-T standard
% Xp=(4/3)*sqrt(2)*(sign(randn(1,NFFT))+ sign(randn(1,NFFT)*1i));
% Xp=(0:NFFT-1)*1i;
% Xp=ones(1,NFFT);
% Xp=1:NFFT;

%%%%%%%%%%%%%%%%%%%%%%%%%%%%%%%%%%%%%%%%%%%%%%%%%%%%%%%%%%%%%%%%%%%%%%%%
%%%%%%%%%%%%%%%%%%%%%%%%%%%%%%%%%%%%%%%%%%%%%%%%%%%%%%%%%%%%%%%%%%%%%%%%
%%%%%%%%%%%%%%%%%%%%%%%%%%%%%%%%%%%%%%%%%%%%%%%%%%%%%%%%%%%%%%%%%%%%%%%%
%%%%%%%%%%%%%%%%%%%%%%%%%%%%%%%%%%%%%%%%%%%%%%%%%%%%%%%%%%%%%%%%%%%%%%%%
% Translate to FFT indices (one based):
% Continual Pilots
kcp=kcp-(Kmax-Kmin)/2; % translate to FFT indices (0 based)
I=find(kcp<0);
kcp(I)=NFFT+kcp(I);
Kcp=ones(68,1)*kcp;

% Scattered Pilots
Ksp=Ksp-(Kmax-Kmin)/2; % translate to FFT indices (0 based)
I=find(Ksp<0);
Ksp(I)=NFFT+Ksp(I);

```

```

% TPS Carriers
ktps=ktps-(Kmax-Kmin)/2; % translate to FFT indices (0 based)
I=find(ktps<0);
ktps(I)=NFFT+ktps(I);
Ktps=ones(68,1)*ktps;

% Nulls
kn=Kmax/2+1:(NFFT-Kmax/2 -1); % translate to FFT indices (0
based)
Kn=ones(68,1)*kn;

% Put all cells together in a matrix Sk 68 x NFFT:
Sk=ones(68, NFFT);
for ell=1:68
    Sk(ell, Kn(ell,:)+1)=0; % mark nulls with 0
    Sk(ell, Kcp(ell,:)+1)=-1; % mark pilots with -1
    Sk(ell, Ksp(ell,:)+1)=-1; % same
    Sk(ell, Ktps(ell,:)+1)=-2; % TPS carriers with -2
end

% FFT (one based) indices for data (Sdata), pilots (Spilots), TPS
(Stps) ,
% nulls (Snulls)

for ell=1:68
    Idata=find(Sk(ell,:)==1); Kdata(ell,:)=Idata;
    Ipilots=find(Sk(ell,:)==-1); Kpilots(ell,:)=Ipilots;
    Itps=find(Sk(ell,:)==-2); Ktps(ell,:)=Itps;
    Inulls=find(Sk(ell,:)==0); Knulls(ell,:)=Inulls;
    Xpilots(ell,:)=Xp(Ipilots); % transmitted pilots
    Xtps(ell,:)=zeros(1,Ntps); % transmitted TPS (not activated)
end
    Xnulls=zeros(68, Nnulls);
% Subcarriers Overhead
Koh=[Kpilots, Ktps, Knulls];
Xoh=[Xpilots, Xtps, Xnulls];

% Modulator mapping from
% [data(68,1512), pilots(68,176), tps(68, 17), nulls(68, 343)]
% to FFT frame subcarriers (one based)
Kmod=[Kdata, Kpilots, Ktps, Knulls];
for i=1:68
    [Ktemp, Ik]=sort(Kmod(i,:));
    Kmod(i,:)=Ik;
end

% Demodulator mapping from FFT subcarriers back to
% [data, pilots, tps, nulls]
for ell=1:68
    [xtemp, I]=sort(Kmod(ell,:));
    Kdem(ell,:)=I;
end

```

```
% end
```

3. Channel Estimation (courtesy Prof. Cristi)

```
function [KH, XpH, IK, Minv]=channelestimator(Kpilots,  
Xpilots,NFFT)  
% [KH, XpH, IK, Minv]=channelestimator(Kpilots, Xpilots, NFFT)  
  
% To test:  
% clear  
% [Kmod, Kdem, Kdata, Xoh, Koh, Nk,NFFT, NCP]=dvbtf2k;  
% Kpilots=Koh(:, 1:Nk(2));  
% Xpilots=Xoh(:, 1:Nk(2));  
  
% 1. Parameters for Channel Freq. Response Estimation by Pilot  
Response Interpolation  
for ell=1:4  
    K0=[Kpilots(ell,:), Kpilots(ell+1,:),  
        Kpilots(ell+2,:),Kpilots(ell+3,:)];  
    X0=[Xpilots(ell,:), Xpilots(ell+1,:),  
        Xpilots(ell+2,:),Xpilots(ell+3,:)];  
    [Ktemp, I]=sort(K0);  
    % eliminate repeated subcarriers due to Continual Pilots  
    K1=K0(I); K1=[K1,NFFT]; % have to add the last  
subcarrier NFFT  
    dK1=diff(K1); I1=find(dK1~=0); % find non repeated  
subcarriers  
    KH(ell,:)=I(I1);  
    XpH(ell,:)=X0(I(I1));  
end  
  
% reorder subcarriers after interpolation  
K1=1:3:853;  
K2=2:3:851;  
K3=3:3:852;  
K4=1197:3:2046;  
K5=1198:3:2044;  
K6=1199:3:2045;  
K7=2047;  
K8=2048;  
K9=854:1196;  
  
K=[K1,K2,K3,K4,K5,K6,K7,K8,K9];  
[Ktemp, IK]=sort(K);  
  
% 2. Matrix for Channel Impulse Response Estimation  
% All pilots values and indices  
Xallp=zeros(1,NFFT);  
for ell=1:4  
    Xallp(Kpilots(ell,:))=Xpilots(ell,:);  
end  
Kallp=[0:3:852, 1196:3:2045]+1;
```

```

% All pilots in time domain
xallp=ifft(Xallp);
% Form matrix
L=64; % max length of channel
X=toeplitz(xallp, [xallp(1), xallp(NFFT:-1:2)]);
X=X(:,1:L);
F2048=ifft(eye(2048)); % ifft matrix
F0=F2048(:, Kallp);
[U,S,V]=svd(X);
L0=55; % number of nonzero singular values we keep
Minv=V(:,1:L0)*diag(1./diag(S(1:L0, 1:L0)))*U(:, 1:L0)'+F0;

% end

```

4. Kalman Filter (courtesy Prof. Cristi)

```

function [num1,num2,den] = kalmaninitial(h1,h2,SDnoise)
coder.extrinsic('ss2tf');
coder.extrinsic('dlqe');

% h1 = h1 / h1(1);
h1 = [h1 0];
h2 = [0 h2];

N1=length(h1);
N2=length(h2);
N=max([N1,N2])-1; % system order

% Form state space matrices
A=[-h1(2:N1)/h1(1);
   eye(N-1), zeros(N-1,1)];
B=[1/h1(1);
   zeros(N-1,1)];
Bw=B;
C=h2(2:N2);
% D = 0;
Q=(SDnoise/h1(1))^2;
R=SDnoise^2;
% Q = 1e-3;
% R = 1e-3;
M = complex(zeros(length(A),1));
[M,P,Z,E]=dlqe(A,Bw,C,Q,R);
K=A*M;
Cx=[zeros(1,N-1),1]; % pick one of the states, say x(n-
N)
%Cx=[1, zeros(1,N-1)]; % pick one of the states, say x(n)
num1 = complex(zeros(length(A)+1,1));
num2 = complex(zeros(length(A)+1,1));
den1 = complex(zeros(length(A)+1,1));

[num1, den1]=ss2tf(A-K*C, B, Cx, 0,1);
[num2, den2]=ss2tf(A-K*C, K, Cx, 0,1);
den = den1;
end

```

THIS PAGE INTENTIONALLY LEFT BLANK

LIST OF REFERENCES

- [1] R. Cristi, M. P. Fargues, and M. Hagstette, "Detection of a weak communication signal in the presence of a strong co-channel TV broadcast interferer," technical report, Department of Electrical and Computer Engineering, Naval Postgraduate School, Monterey, CA, October 2013.
- [2] M. Hagstette, "Extraction of a weak co-channel interfering communication signal using complex independent component analysis," M.S. thesis, Department of Electrical and Computer Engineering, Naval Postgraduate School, Monterey, CA, 2013.
- [3] S. Dessalermos, "Adaptive reception for underwater communications," Ph.D. dissertation, Department of Physics, Naval Postgraduate School, Monterey, CA, 2011.
- [4] M. Aydogmus, "Multireceiver acoustic communications in time-varying environments," M.S. thesis, Department of Electrical and Computer Engineering, Naval Postgraduate School, Monterey, CA, 2014.
- [5] DVB Worldwide. (n.d.). Digital Video Broadcasting Project Office. [Online]. Available: <https://www.dvb.org/news/worldwide>.
- [6] "Multi carrier modulation and OFDM," class notes for EC4910 Digital Signal Processing for Communications, Department of Electrical and Computer Engineering, Naval Postgraduate School, Monterey, CA, Fall 2014.
- [7] T. T. Ha, *Theory and Design of Digital Communication Systems*. New York: Cambridge University Press, 2011, ch. 6, sec. 18, pp. 282–290.
- [8] W. Zhang, Y. Guan, W. Liang, D. He, F. Ju, and J. Sun, "An introduction of the Chinese DTTB standard and analysis of the PN595 working modes," *IEEE Trans. Broadcast.*, vol. 53, no 1, 2007, pp. 8–13.
- [9] *Digital Video Broadcasting (DVB); Frame Structure Channel Coding and Modulation for a Second Generation Digital Terrestrial Television Broadcasting System (DVB-T2)*, European Standard ETSI EN 302 755 V1.3.1 (2012-04), 2012.
- [10] Y. B. Shalom, X. R. Li, T. Kirubarajan, *Estimation with Applications to Tracking and Navigation*. New York: Wiley Interscience, 2001.

THIS PAGE INTENTIONALLY LEFT BLANK

INITIAL DISTRIBUTION LIST

1. Defense Technical Information Center,
Ft. Belvoir, Virginia
2. Dudley Knox Library
Naval Postgraduate School
Monterey, California